UNIVERSITY OF MICHIGAN

Optimal Design of an RC Aircraft for Payload-Bearing Missions

by

Rakesh Jayakumar
Jianxin Li
Mohit Mehendale
David Moiseev

ME 555-2011-08
Winter 2011 Final Report

ABSTRACT

This optimization study aims to maximize the payload-bearing capacity of a remote-controlled (RC) monoplane with a conventional T-tail configuration. The design of this aircraft will be limited by the dimensional and performance constraints listed in the Rules document of the Society of Automotive Engineers (SAE) Aero Design 2011 competition, and also by inherent aircraft properties that allow for a safe flight. The results of this optimization study are likely to lie exactly on the dimensional constraints (5.715m in total dimensions) specified, because as a general rule of thumb, the largest feasible (i.e. stable) design should be able to produce the maximum amount of lift. The optimal result should also feature minimal structural weight such that the payload-bearing capacity of the aircraft is maximized.

Table of Contents

1 Introduction 3
2 Subsystems 5
2.1 Aerodynamics Subsystem (by Jianxin Li) 5
2.1.1 Problem Statement 5
2.1.2 Nomenclature 6
2.1.3 Mathematical Model 7
2.1.4 Model Analysis 11
2.1.5 Optimization Study and Numerical Results 11
2.1.6 Parametric Studies 14
2.1.7 Discussion of Results 14
2.2 Structures Subsystem (by David Moiseev & Rakesh Jayakumar) 14
2.2.1 Problem Statement 14
2.2.2 Nomenclature 14
2.2.3 Mathematical Model 15
2.2.4 Model Analysis 22
2.2.5 Optimization Study 23
2.2.6 Parametric Studies 26
2.2.7 Discussion of Results 26
2.3 Landing Gear Assembly Subsystem (by Mohit Mehendale) 28
2.3.1 Problem Statement 28
2.3.2 Nomenclature 29
2.3.3 Mathematical Model 30
2.3.4 Model Analysis 33
2.3.5 Optimization Study 33
2.3.6 Parametric Study 35
2.3.7 Discussion of Results 35
3 System 36
4 Acknowledgements 39
5 References 39
Appendix A: Aerodynamics MATLAB Scripts & EGO Set-Up 40
Appendix B: Structures Subsystem Results 44
Appendix C: System Level Results 47
Appendix D: System Level Results 2 49

1 Introduction

With the aim of representing the University of Michigan at the college-level SAE Aero Design 2012 competition, our team will be looking into maximizing the payload (overall system-level objective) that an RC aircraft with a conventional configuration can carry, designed within the competition's rules. The conventional layout is shown in Figure 1 below (without the wing tip devices).

Figure 1: Conventional aircraft configuration.

This configuration was chosen based on its straightforwardness in terms of geometry, as our team is largely inexperienced in conducting design-related optimization work. Should time permit within the length of this course, we will expand to conduct optimization over even more design variables that will allow us to venture beyond this basic configuration.

In designing an aircraft intended for maximum load-bearing capacity, intuitively, the structural weight of such an aircraft has to be kept as low as possible due to dimensional limitations on lifting surface area that result in limitations on the lift force produced. However, the aircraft still has to possess sufficient structural integrity to withstand the static and dynamic loads it will be subjected to in the course of its flight that can be split into three main stages – take-off, cruise and landing. As it has to remain dynamically stable and controllable at all times, its control surfaces will have to be of a minimum area despite efforts to reduce overall structural weight. This becomes an optimization problem in which the effective load-bearing capacity of the aircraft has to be maximized, subjected to inherent performance constraints necessary for a safe

flight, and further constraints on aircraft dimensions and material properties (no fiber-reinforced materials allowed) as imposed by the competition rules.

M-Fly, a University of Michigan student team under the Aerospace engineering department, participates in this competition annually and has previous designs that have successfully flown at this competition, albeit under different (primarily) dimensional rules. For the initial phase of this project, we will be leveraging extensively on M-Fly's experience in designing such an aircraft, most notably, in obtaining a feasible design to initialize the optimization.

The subsystems of such an aircraft can be decomposed into: Aerodynamics, Structures and Landing Gear Assembly, as is done traditionally for conventional aircraft. The Structures team, due to the larger amount of effort required in modeling the critical 'lifting' components of the aircraft, is further decomposed into the main wing, fuselage plus empennage components.

The individual subsystems are linked as such: in the Aerodynamics subsystem, the lift force generated by the main wing is to be maximized by varying the main wing and empennage (for control) geometries. The aerodynamic analyses to be conducted are inherently dependent on the structural weight of the aircraft – such as the main wing, empennage, fuselage and landing gear assembly, especially in feasibility/stability evaluations. In the Structures subsystem, the Finite Element Analyses (FEA) to be conducted on the aircraft model is predicted to be an active constraint in the minimum structural weight configuration (optimal). The results of the FEA is highly-dependent on the distributed load (i.e. lift force) acting on the main wing. Similarly, in the Landing Gear Assembly subsystem, the structural weight of the assembly is to be minimized so as to minimize the overall structural weight of the aircraft. But in this subsystem, the constraints are different from the main Structures subsystem because the landing gear is subjected to distinctly different loading conditions (when compared to the aerodynamic surfaces) both statically and dynamically.

Independent improvement of the design of each subsystem will not necessarily lead to an overall optimum aircraft configuration; however, it will be in proximity of the optimal solution and it is expected to yield the optimum configuration after minor modifications to the values of the design variables/subsystem-specific parameters. This is because fundamentally, the objective in each

subsystem contributes directly towards the overall system objective of maximizing payload-bearing capacity.

2 Subsystems

The following sub-sections will outline the individual subsystems and their respective optimizations in further detail. The Aerodynamic subsystem was the responsibility of Jianxin Li. The Structures subsystem was the responsibility of David Moiseev and Rakesh Jayakumar. The Landing Gear subsystem was the responsibility of Mohit Mehendale.

2.1 Aerodynamics Subsystem (by Jianxin Li)

This subsystem is primarily concerned with the design of the aerodynamic surfaces of the aircraft, namely the main wing and empennage system, such that the aerodynamic forces acting on the aircraft are the most desirable for maximum payload-bearing capacity.

2.1.1 Problem Statement

The Aerodynamics subsystem aims to improve the overall payload-bearing capacity of the aircraft by maximizing the amount of lift force that the main wing is able to generate. Intuitively, to generate more lift, wing span and area are to be increased. However, there is a limit to the wing span due to dimensional restrictions of the competition. Also, an increase in lift is typically accompanied by an undesirable increase in drag force due to the increased surface area, and this will affect the ability of the aircraft to take off within 60.96m (another competition requirement). Hence the tradeoff between additional lift and drag forces has to be studied and taken into consideration.

In this subsystem, we used Nicholai's method [1] of simulating runway take-off in a MATLAB script and conducted aerodynamic analyses using Athena Vortex Lattice (AVL), an open-source software commonly used by students for aerodynamic analyses.

2.1.2 Nomenclature

The symbols involved in this subsystem are listed below.

Table 1: Nomenclature used in Aerodynamics subsystem.

W_T = total weight of aircraft

L = lift force generated by wing of aircraft

D = drag force acting on aircraft

c_L = coefficient of lift of aircraft

c_{L_TO} = coefficient of lift of aircraft at take-off

c_{L_max} = maximum coefficient of lift of aircraft

c_D = coefficient of drag of aircraft

V = airspeed (velocity)

ρ = air density

φ = set of points in root locus plot

d_{TO} = take-off distance (runway)

SM = static margin

h_{LG} = height of landing gear

f_{rad} = radius of fuselage

l_{fuse} = length of fuselage

x_W = distance from nose to wing leading edge

x_V = distance from nose to horizontal tail leading edge

x_H = distance from nose to vertical tail leading edge

b_W = wing span (main wing)

b_V = vertical tail span

b_H = horizontal tail span

S = planform area of main wing

c_W = chord length at wing root (center)

c_V = vertical tail chord length

c_H = horizontal tail chord length

f_{ail} = fraction of wing span to be used for aileron

f_{rud} = fraction of wing span to be used for rudder

f_{ele} = fraction of wing span to be used for elevator

2.1.3 Mathematical Model

This sub-section presents the scientific relations between the parameters and variables to be used in the optimization process.

2.1.3.1 Objective Function

The objective of the Aerodynamics subsystem is to maximize the lift force that the aircraft is capable of producing during cruise. Since lift is primarily generated by the main wing of the aircraft, it can be expressed in terms of variables that describe the geometry and properties of the main wing. A general way of calculating lift [2] is:

$$L = \frac{1}{2}\rho V_{TO}^2 S c_L$$

For our monoplane with a conventional 'rectangular' wing configuration without taper (for ease and accuracy in construction), the wing surface area can be calculated using $S = b_W c_W$. Also, from M-Fly's previous design experiences, the lift requirement for the take-off phase is the most difficult to achieve as the aircraft will need to accelerate from 0m/s to V_{TO} on a limited runway length and engine thrust. This imposes the most stringent lift requirement on the aircraft. Thus, the lift should be maximized based on the take-off phase as such:

$$L = \frac{b_W c_W}{2}\rho V_{TO}^2 c_{L\_TO}$$

c_{L_TO} will be calculated in AVL based on the input file that contains the main wing geometry (involves b_W and c_W) as well as the airfoil used. V_{TO} is calculated by equating L to W_T and solving the above equation for V_{TO} (with only $0.8c_{L\_max}$ available [1] to account for environmental factors) as such:

$$V_{TO} = \sqrt{\frac{2W_T}{b_W c_W \rho\ 0.8 * c_{L\_max}}}$$

ρ is actually a constantly-changing environmental factor during flight, but for the purposes of this optimization study, ρ will be a parameter fixed at 1.13437kg/m^3 based on a typical flying altitude of 100m and temperature of 20°C.

2.1.3.2 Constraints

First and foremost, the aircraft will have to be capable of producing sufficient lift (i.e. more than total aircraft weight) at the end of the 60.96m runway to be able to take-off. Therefore, the total aircraft weight acts as a lower bound on lift as such:

$$W_T \leq L = \frac{b_W c_W}{2} \rho V_{TO}^2 c_{L\_TO}$$

Based on the basic physical constraints (in terms of manufacturability/feasibility) on the geometric variables, we have:

$$b_W, b_V, b_H, c_W, c_V, c_H, f_{ail}, f_{rud}, f_{ele} > 0.1$$

Non-negativity of aerodynamic variables is already enforced in the aerodynamic solver, i.e. the solver will not produce a c_L value that is negative based on the airfoil we have chosen to use. Practical engineering constraints impose another set of bounds on the variables. V_{TO} is upper-bounded by the amount of effective thrust that the engine is capable of producing for the aircraft (since the engine model is fixed under competition rules), and this in turn is affected by total aircraft weight. This constraint is already accounted for in the MATLAB take-off simulation code (Appendix A), in which take-off runway length (d_{TO}) is required to be no more than 60.96m:

$$d_{TO}(all\ design\ variables) \leq 60.96m$$

The wing's coefficient of lift (c_L) is constrained by the airfoil's maximum coefficient of lift (c_{l_max}) at stall conditions; it would not make sense to design wing with a lift coefficient that exceeds what its individual sections (airfoil) are capable of without stalling. Thus, the lift coefficient of the airfoil places an upper bound on the lift coefficient of the wing as such:

$$c_L \leq c_{l\_max} = 2.4$$

The high-lift airfoil with a reasonable range of pre-stall angle of attack chosen for this aircraft is the Eppler E420 with a maximum lift coefficient of 2.4 right before a stall angle of 15°.

Next, for the aircraft to fly safely or pass safety inspection at the competition, it has to be statically and dynamically stable while in flight. Static stability is determined by the static margin calculated based on the moments generated by the aerodynamic forces and the weight of the aircraft, hence its value depends on the weight of the aircraft and its aerodynamic properties, thereby dependent on the geometric variables of the aerodynamic surfaces. The static margin can be computed in AVL and subsequently extracted for analysis. For an aircraft of its class, usually a static margin of at least 0.10 (10%) is required for it to be considered stable, resulting in the following constraint:

$$\text{SM} = \text{fn}(all\ design\ variables) \geq 0.10$$

Dynamic stability can be assessed by analyzing the Real components of the aircraft's Root Locus Plot. The points on this plot and their respective coordinates are calculated based on aircraft stability derivatives, which in turn are dependent on aircraft geometry and weight; these coordinates can be extracted from AVL for further analyses as well. For an aircraft to be considered dynamically stable, the Real components of these points have to be negative. We let φ denote the set of coordinates for the points on the Root Locus Plot, and we will require:

$$\mathrm{Re}(\varphi) = \mathrm{fn}(\textit{all design variables}) \leq 0$$

Lastly, competition design rules restrict the three dimensions of the aircraft to 5.715m and below, resulting in the following constraint:

$$b_W + h_{LG} + f_{rad} + l_{fuse} \leq 5.715\text{m}$$

This therefore limits the available wing span (b_W), as sufficient vertical tail/rudder height (b_V) and ground clearance from landing gear assembly is necessary for a safe flight defined as a stable flight.

2.1.3.3 Design Variables and Parameters

Based on M-Fly's previous aircraft analyses, design variables for the Aerodynamics subsystem and their respective values used as a 'starting point' in this optimization study are:

Table 2: Values used for the design variables as a feasible starting point.

Variable	Value
b_W	2.90m
b_V	0.305m
b_H	0.305m
c_W	0.400m
c_H	0.223m
c_V	0.223m
x_W	0.600m
x_H	1.78m
x_V	1.91m
f_{ail}	0.8
f_{rud}	0.8
f_{ele}	0.8

As such, there will be 12 degrees of freedom in this subsystem.

The parameters and their respective values are:

Table 3: Parameters used in the Aerodynamics subsystem.

Parameters	Value
ρ	1.1343kg/m^3
V_{TO}	10.88m/s
W_T	155N
c_{l_max}	2.4
l_{fuse}	2.13m
h_{LG}	0.1m

These values correspond to give a starting objective function value of $\underline{L = 155\text{N}}$ (using c_L=c_{l_max}).

2.1.3.4 Summary Model

In essence, the optimization problem of the Aerodynamics subsystem is as follow:

$$\text{Max.} \quad L = \frac{b_W c_W}{2} \rho V_{TO}^2 c_{L\_TO}$$

$$\text{s.t.} \quad b_W + b_V + h_{LG} + f_{rad} + l_{fuse} \leq 5.715\text{m}$$

$$d_{TO} = \text{fn}(\textit{all design variables}) \leq 60.96\text{m}$$

$$W_T \leq \frac{b_W c_W}{2} \rho V_{TO}^2 c_{L\_TO}$$

$$c_L \leq c_{l\_max}$$

$$\text{SM} = \text{fn}(\textit{all design variables}) \geq 0.10$$

$$\text{Re}(\varphi) = \text{fn}(\textit{all design variables}) \leq 0$$

$$b_W, b_V, b_H, c_W, c_V, c_H, f_{ail}, f_{rud}, f_{ele} > 0.1$$

Converting to negative-null form:

$$\text{Min.} \quad -L = -\frac{b_W c_W}{2} \rho V_{TO}^2 c_{L\_TO}$$

$$\text{s.t.} \quad b_W + b_V + h_{LG} + f_{rad} + l_{fuse} \leq 5.715\text{m}$$

$$[d_{TO} = \text{fn}(\textit{all design variables})] - 60.96\text{m} \leq 0$$

$$W_T - \frac{b_W c_W}{2} \rho V_{TO}^2 c_{L\_TO} \leq 0$$

$$c_L - c_{L\_max} \leq 0 \text{ (sectional span-wise)}$$

$$0.10 - [\text{SM} = \text{fn}(\textit{all design variables})] \leq 0$$

$$\text{Re}(\varphi) = \text{fn}(\textit{all design variables}) \leq 0$$

$$0.1 - (b_W, b_V, b_H, c_W, c_V, c_H, f_{ail}, f_{rud}, f_{ele}) \leq 0$$

2.1.4 Model Analysis

Based on the analytical expressions from above, monotonicity analysis was conducted and the results are presented in the following table:

Table 4: Monotonic relationships within the Aerodynamics subsystem

Function/Variables	b_W	b_V	b_H	c_W	c_H	c_V
$-L$	-			-		
$b+h+l$	+					
d_{TO}	U^+			U^-		
W_T - L	-			-		
c_L-c_{L_max}				U^+		
SM	U^-	U^+	U^+	U^+	U^+	U^+
Re(φ)		U^-	U^-		U^-	U^-

The rows in grey indicate constraint functions that will be calculated and solved for in AVL and MATLAB and are too complex to be presented here analytically, these functions tend to have intermediary aerodynamic variables calculated in AVL as inputs.

Based on the monotonicity analysis, the 3-dimension constraint of $b_W + b_V + h_{LG} + f_{rad} + l_{fuse} \leq$ 5.715m will certainly be active (effect of U^+ is considered *un*certain at this point). This matches pre-analysis intuition because in order to achieve maximum lift, maximum possible wing span will be required and consequently, it will be accompanied by the bare minimum rudder span (b_V) such that the aircraft remains controllable (i.e. $\text{Re}(\varphi) \leq 0$ is satisfied). After the elimination of several intermediary variables/constraints through monotonicity analysis, we end up with a problem that is well-bounded (as shown above) as each function is bounded from above and below by at least one other constraint function.

2.1.5 Optimization Study and Numerical Results

The optimization was conducted with MATLAB as the main program in which commands were scripted to – for interfacing with AVL, conducting intermediary calculations (for objective function and constraints' values) and optimization (used *fmincon*). A flow chart showing the processes used is shown as follows:

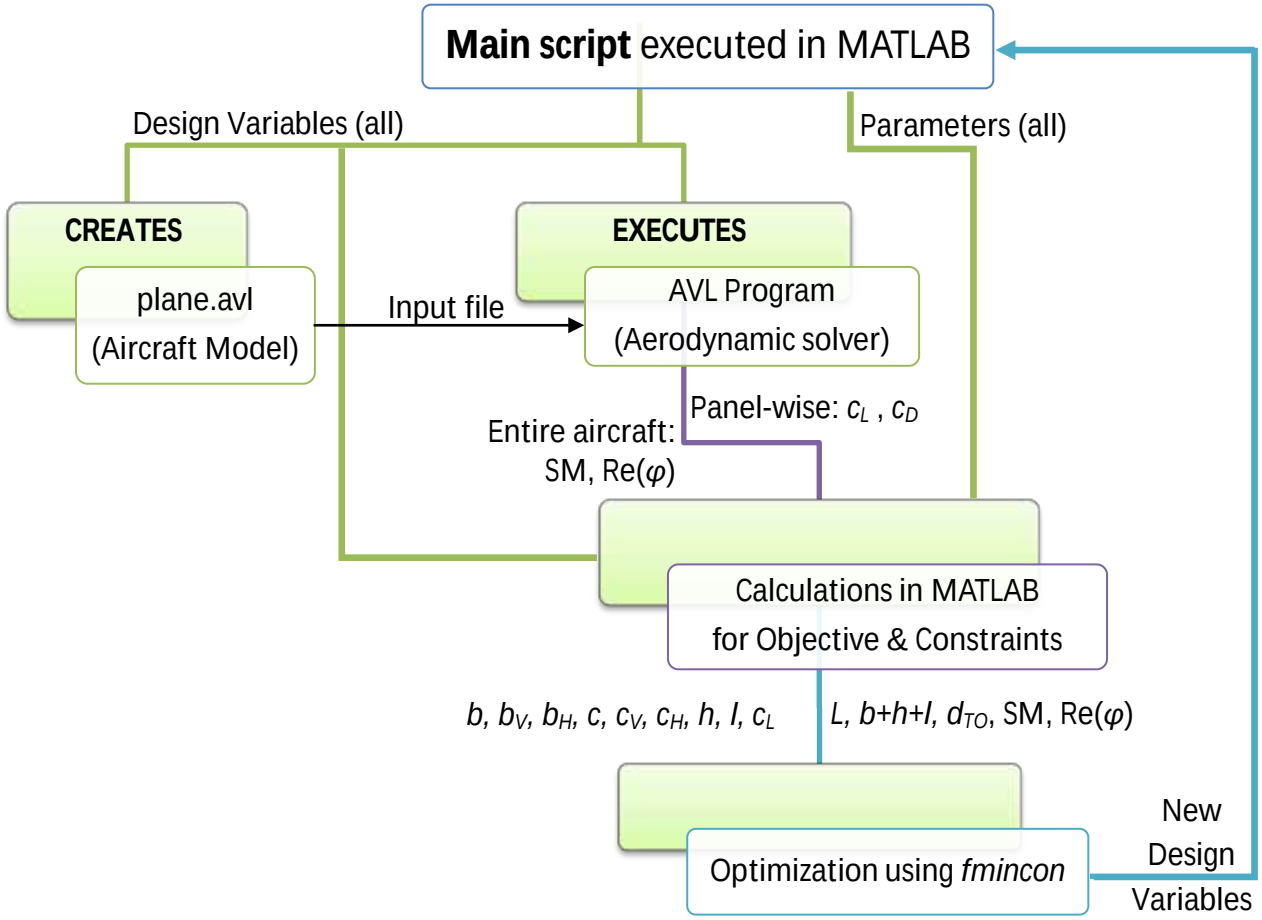

Figure 2: Aerodynamic sub-system flow chart.

From using *fmincon*, the maximum lift achievable by a monoplane with a conventional design is 213N (compared to the starting 155N), based on the following values of the design variables:

Table 5: Comparison of the values of the design variables.

Variable	Initial Value	Optimized Value
b_W	2.90m	2.64m
b_V	0.305m	0.745m
b_H	0.305m	0.894m
c_W	0.400m	0.275m
c_H	0.223m	0.100m
c_V	0.223m	0.100m
x_W	0.600m	0.637m
x_H	1.78m	2.02m
x_V	1.91m	2.03m
f_{ail}	0.8	0.9

f_{rud}	0.8	1
f_{ele}	0.8	0.5

The optimal solution is constraint-bound, as evidence by the following constraint values obtained at the optimal point:

Table 6: Comparison of the values of the constraint functions.

Constraint	Initial Value	Optimized Value
$c_L - c_{L\_max}$	0.2	**0**
SM	0.15	**0**
$d_{TO} - 60.96$	-32.55m	-0.0007m
$W_T + L$	-5N	-63.3N
Re(φ)	All negative	All negative

The active constraints at the optimal point are highlighted in blue. The only inactive constraints were the stall requirement and the static stability requirements.

As most of the constraints turned out to be active, the result is largely a constraint-bound optimum point. Relating constraint activity to predictions based on the monotonicity analysis conducted, the constraint on the 3-dimensions and one component of Re(φ) indeed turned out to be active, with the final results showing activity beyond the prediction, which was expected since the monotonicity analysis could only be conducted to a limited extent due to the non-analytical nature of the problem.

Global convergence was achieved by creating a hypercube using the EGO algorithm (Appendix A), followed by SQP minimization using the 'minimum' point identified by EGO. Different starting points (i.e. different 'low' points in the EGO-generated hypercube) were used in the SQP to validate the global minimum.

Scaling did not prove to be an issue as most of the function evaluations, when done properly (i.e. equations were rearranged to avoid division by zeros or small numerical errors), were within the range of 0.001 to about 200 (numbers of this order were only involved in terms of forces).

It should be noted that only up to 3 decimal places were necessary for the geometric variables, as anything more will be beyond manufacturable/measurable precision based on the current tools

that M-Fly has. Hence, the error tolerance for convergence is only necessary up to 10^{-3} and this sped up the optimization process significantly.

2.1.6 Parametric Studies

The subsystem was further tested with by varying W_T , an important driver that will dictate results in this subsystem and a main factor that is largely dependent on the optimization results of the remaining two subsystems.

As W_T increased, the amount of Lift the aircraft can be designed to produce decreases. This is because increasing W_T violates the SM, Re(φ) and d_{TO} constraints and in order to counter these violations, L has to be decreased and the 3-dimensions constraint becomes active. This later proved to be an important driver in the system-level integration process.

2.1.7 Discussion of Results

The optimal results make physical sense, however, it was unexpected that the stability and stall constraints proved to be more challenging to satisfy. Also, the reduction in wing span and chord lengths imply that the effect of drag forces decrease the benefits of having larger lifting surfaces, in turn implying that drag effects are more prominent that we believed prior to conducting optimization.

2.2 Structures Subsystem (by David Moiseev & Rakesh Jayakumar)

This subsystem is primarily concerned with the design of the crucial aerodynamic structures of the aircraft, such as the main wing and the empennage.

2.2.1 Problem Statement

It is important to identify an optimized structure of the plane so that it can withstand the necessary loading forces and stresses. The objective of the subsystem was to minimize the mass of the structure by analyzing the structural integrity using loads, stresses and buckling constraints that would be applicable. The model variables have been changed to minimize discretization and reduce computation time in an F.E.A environment. Variables such as number of ribs and spars have been made as parameters. As the model was made on C.A.D, it was difficult to create an iterative process that would introduce new parts in the structure. All variables in the math model are dimensions that can vary.

2.2.2 Nomenclature

The variables and parameters as per the updated model are listed below:

b = wing span (P)

C_W = wing chord length (P)

C_V = vertical tail chord length (P)

C_H = horizontal tail chord length (P)

Wt_S = weight of structure (V)

Wt_p = weight of payload (P)

Wt_F = weight of fuel (P)

Wt_{LG} = weight of landing gear assembly (P)

L = lift force generated by wing of aircraft (P)

S_r = spacing between ribs (V)

N_s = number of spars (C)

N_r = number of ribs (C)

t_r= thickness of ribs (V)

A_r = area of the rib from the aero-foil structure (P)

Ws1= width of front spar(s) (V)

Ws2= width of rear spar(s) (V)

H_{s1}= height of front spar(s) (V)

H_{s2}= height of rear spar(s) (V)

2.2.3 Mathematical Model

This sub-section presents the scientific relations between the parameters and variables to be used in the optimization process.

2.2.3.1 Objective Function

The objective is to minimize the weight of the structure Wt_s. The weight of the structures can be divided into the three individual weights: fuselage, empennage and the wings. The structure weights for both the wings and the empennage are independent of the other. Due to complexity and shortage of time only the wings were considered in the structure. The weight of the empennage and the fuselage are assumed as parameters for the system optimization. The objective is derived as a summation of the weight of all the individual components i.e ribs and the spars that are used in the structure.

Obj: $\min(Wt_s)$

$Wt_s = F\ (B_s, H_s, tr, W_s, b,\ C_W, C_V, C_H) =$

Wing weight

Wt_s= mass * Density of balsa wood * g

$$\text{mass} = F(\text{Tr}, \text{Hs}_1, \text{Hs}_2, \text{Ws}_1, \text{Ws}_2, \text{AllParameters})$$

The mass is calculated by Abaqus directly and sent as output.

2.2.3.2 Constraints

$$Wt_s - (L/(S.F) - Wt_p + Wt_f + Wt_{Lg} + Wt_e) \leq 0$$

Weight of the entire plane should be less than the lift to take off with accountability for variations in the atmosphere. Hence weight of the structure should be less than the lift minus the weight of the rest of the plane. This is an in-active constraint and hence was not taken into consideration during the optimization of the sub-system, but will be important for the over-all system.

General stress constraint in-order to define structural integrity. It will be evaluated for all the ribs and the spars along with a factor of safety.

$$\sigma = F\ (N_r, N_s, tr, b,\ C_W, C_V, C_H, Ws1, Ws2, Hs1, Hs2\ A_r, S_r)$$

Stress analysis was conducted based on F.E.A. on Abaqus for the wing structure. The finite element model shown in figures 3 and 4 is a full 3-d model utilizing two types of solid elements TET-10 and HEX-20 from Abaqus. The geometry for the model was created solely using python. This allowed for great flexibility in the model. However the model that we have completed up till this point is much too complicated for optimization, in order to reduce time per solution a simpler model using beam and shell elements. In addition to a reduction in time per solution overall model complexity will be reduced; A reduction from 20 minutes, 3D, to 2 minutes, 2D. The loading cases and boundary conditions will not change. Currently we are only finding results for a load case involving lift. The load is being applied to the top surface of the top spars; it is a pressure load that has a total force of 20 pounds. The load value is taken from the load cases used by M-Fly in their competition design report. The current boundary condition is to fix, in 6 degrees of Freedom (DOF), the inner surface of the 1st rib. This boundary condition is not realistic, however it is reasonable. A more accurate boundary condition could be the inner surface of the 1st rib will have a symmetry boundary condition and the ribs that are over the

fuselage will have the bottom edge fixed in all 6 DOF. This models a possible way the wing could be attached to the rest of the plane.

The model used in the final optimization run, shown in figure Y, is a simple beam and shell model. Any geometric parameter or variable will cause a change in the Abaqus model appearance this flexibility will help with the system optimization. The model went through a difficult debugging process, this process was needed to ensure that the optimization possess would not break down. The run time for each iteration is approximately two minutes.

Equality constraints

$$H_1: \quad 0 = \mathrm{Nr} * \mathrm{tr} + \sum_{i=1}^{\mathrm{Nr}} \mathrm{Sr}_i - \mathrm{b}$$

The equality constraint H_1 is the general form. H_1 ensures that the wing will never (as a result of the variable spacing function) become longer or shorter than the specified wing span. This constraint was implemented in the modeling code to ensure that it would never be violated and to reduce degrees of freedom. The constraint was implemented in two ways, one for the solid model case and another for the beams and shells model. The primary difference is that in the solid model the thickness of the ribs (t_r) is a concern.

For the solid model, the center front tip of each rib was defined as the part coordinate frame origin and when spaced the ribs move based on the center point instead of their side. The only exception was to slide the first and last rib inward by half the rib thickness. Otherwise the method selected to implement, constraint H_1, was the same for both models.

$$\mathrm{ac}_2 x^2 + \mathrm{ac}_1 x = \mathrm{CenterOfRib} \qquad (1)$$

$$\mathrm{ac}_2 = \mathrm{a}_2 * \mathrm{b} \qquad (2)$$

$$\mathrm{ac}_1 = \mathrm{b} \qquad (3)$$

The ribs were spaced unevenly; this helps to increase the maximum buckling load. This is true because buckling in a beam is inversely proportional to the length between its supports. A quadratic function was selected due to its simplicity; but other functions may be better suited to define the implementation and reduce the number of variables needed. The function used to space the ribs, eq.# 1 needs the constraint H_1 in order to produce a valid wing. When x, in eq.# 1,

is defined as a set of evenly spaced numbers between 0 and X_{upper}; the sets has the same number of elements as there are ribs. This gives results such as the one shown in Figure 3.

$$X_{upper} = \begin{cases} \frac{-1+\sqrt{1^2+4a_2}}{2a_2} & , \quad \text{if } a_2 \neq 0 \\ 0 & , \quad \text{if } a_2 = 0 \end{cases} \quad (4)$$

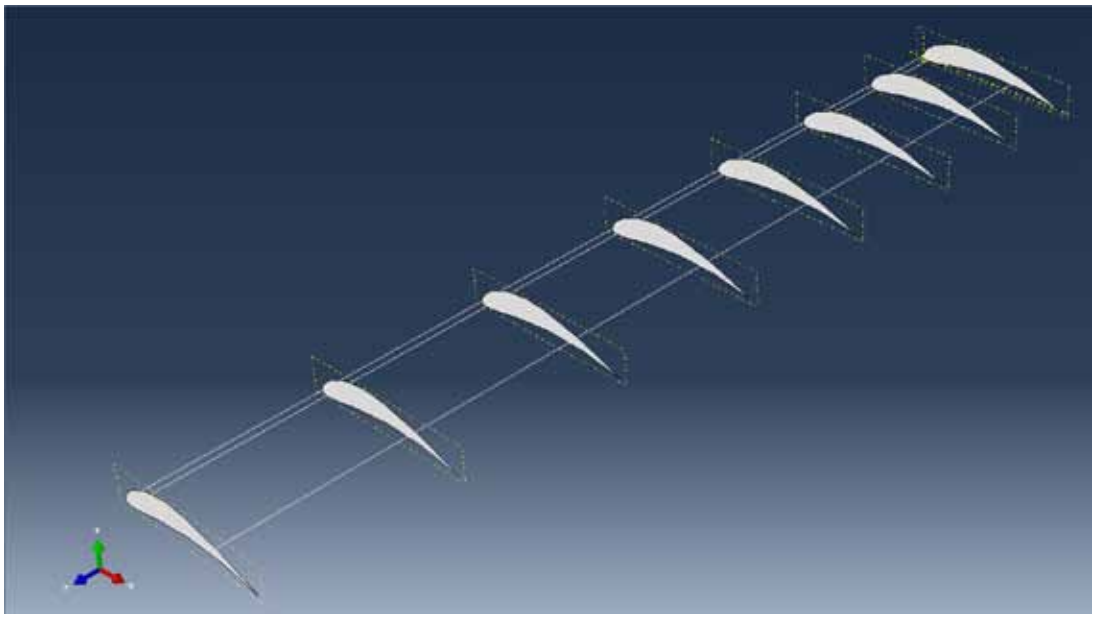

Figure 3: Rib spacing for $a_2 = 2$

Inequality constraints

Stress Constraint

The stress constraint is G_1, in order to find the maximum Von Mises stress. The stress was found using the standard static non-linear solver in Abaqus.

$$G_1: -\frac{\sigma_y}{\text{FactorOfSaftey}} + \text{MaxMises} \leq 0$$

During this step the mass was also calculated based on the finite element mesh, since a course mesh was used the mass is only an estimate but should be very close. A slightly finer mesh would be preferred in the ribs; but the iteration time would have become too long. In order to increase the solving speed for full system optimization, individual mesh controls might be implemented for ribs and spars for improved speed. The young's modulus Poisson's ratio and yield stresses were all taken are mentioned in Table 7.

Table 7: Material properties.

Young's modulus (E)	550000 psi
Poisson ratio (ν)	.1
Yield Stress (σ_y)	3000 psi
Density (ρ)	.0056 Lbf/in^3

Buckling Constraint

$$G_2: -\text{FactorOfSaftey} + |\lambda_1| \leq 0$$

In addition to the failure in either purely tension or compression, the structure can also fail in buckling. The subspace eigen-buckling solver in Abaqus was used; a non-linear analysis was conducted due to the large displacements that occur in the wing. While the non-linear analysis does increase solution time it gives a more accurate result which is especially noticeable when there are large displacements. The eigenvalue λ_1 is related to load by eq. #5. This shows that if the eigenvalue is less than 1 then the structure will fail under the given load. Thus in order to not fail in buckling with a factor of safety the λ_1 must be greater than the factor of safety.

$$\text{bucklingLoad} = \text{load}\,\lambda_i \quad (5)$$

$$\lambda_i = F(\text{AllVaribles}, \text{AllParameters})$$

Displacement/Rotation Constraint

The shape of the wing is important, as deformation can cause the airplane to lose lift, stability or controllability. Based on standard design the wing should handle up to 6° of deflection in the geometric twist Figure 4 and the deviation from the prescribed dihedral angle Figure 5. However using a factor of safety of 2, a tolerance of 3° was applied to constraints G_3 and G_4 respectively.

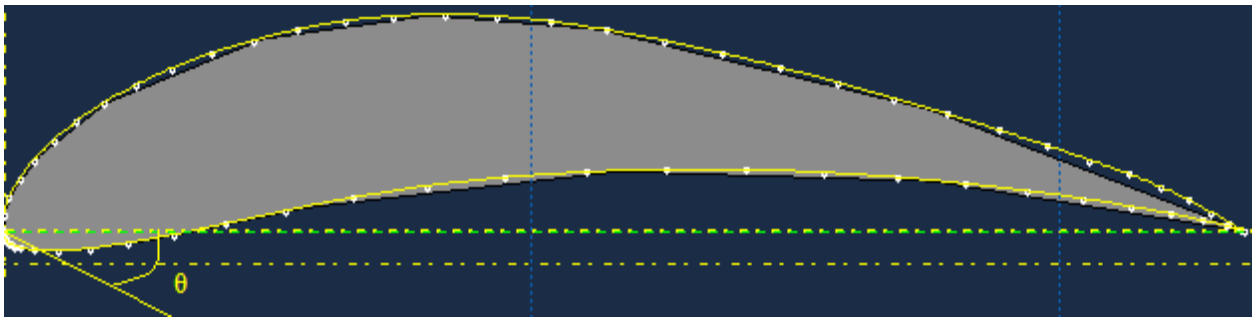

Figure 4: Where θ is defined as geometric twist.

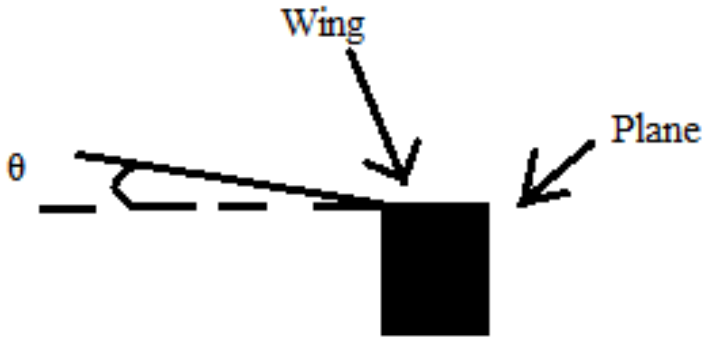

Figure 5: Where theta is defined as the dihedral angle.

$$G_3: -\text{ArcTan}\left(\frac{|\text{YdisplacmentMax}|}{\text{wingSpan}}\right) + 3 \leq 0$$

$$G_4: -|\text{RotationZMax}| + 3 + \text{geometricTwist} \leq 0$$

By the nature of the loading case the maximum displacement must always occur at the tip of the wing. It is safe to assume that the constraints will accurately describe the actual deformation without necessarily using the same point or node ever time.

Rib Spacing Constraints

Constraints G_5through $G_{11}$are rib spacing constraints; z_i is the center of each rib. A spacing larger than 12 inches between the ribs will cause deformation of the skin, due to the shearing and normal effects of the air flow. In cases where there are more constraints than are needed negative one is assigned to the extra constraints (i.e. when Nr / Ns is changed.)

$$G_{5-11}: -(12 - z_{i+1} + z_i) \leq 0 \quad \text{or} \quad S_r - 12" \leq 0$$

Table 8: Variables and their nominal values.

Variable	**Nominal** (Before EGO / AFTER EGO)
A_2(Ribs spacing quadratic term)	.5 / 1.25
Tr (Rib thickness)	.5 / 1.25
Hs_1 (Front rib height)	.2 / .1
Ws_1 (Front rib width)	2 / 1.962
Hs_2 (Back rib height)	.25 / .534
Ws_2 (Back rib width)	.25 / .745

Dimensional constraints

The dimensional constraints were selected based on available material. They serve as bounds for the variables.

$$G_{12}: -t_r + 0.1" \leq 0$$
$$G_{13}: -Ws1 + 0.4" \leq 0$$
$$G_{14}: -Ws2 + 0.4" \leq 0$$
$$G_{15}: -Hs1 + 0.4" \leq 0$$
$$G_{16}: -Hs2 + 0.4" \leq 0$$

2.2.4 Model Analysis

Monotonicity tables, description of activity.

Table 9: Monotonicity and activity.

	Ws1	Ws2	Hs1	Hs2	tr	a2	Activity
f(Ws)	+	+	+	+	+		
G1	-	-	-	-	-		Unknown
G2	U	U	U	U		U	Unknown
G3			U	U			Unknown
G4	U	U	U	U	U		Unknown
G5						U	Unknown
G6						U	Unknown
G7						U	Unknown
G8						U	Unknown
G9						U	Unknown
G10						U	Unknown
G11						U	Unknown
G12					-		Unknown
G13	-						Unknown
G14		-					Unknown
G15			-				Unknown
G16				-			Unknown

The objective function is dependent on all but one variable. The constraints G_1- G_4 are the loading, buckling and twist constraints. The Abaqus FEA solver calculates the values for each of these based on the variables. These constraints use the outputs such stress, displacement, rotation from Abaqus. The lack of specific dependency is hard to identify. Even though the activity is unknown, these equations can serve as lower bounds for the dimensional variables as they indicate loading conditions.

Constraints G_5-G_{11} serves as upper bounds for the spacing between the ribs. As the wing length is smaller than 12 inches times Nr, there is a very high possibility of all or majority of these constraints being in-active. The final set of constraints which are G_{12} to G_{16} are dimensional in nature. They again serve as the lower bound for the variables. The activity cannot be found by simple monotonic analysis, due to the presence of the stress constraints whose activity is also unknown.

Scaling was done on a good number of constraints with factors varying from 10-1000. This was done as both Optimus and Abaqus have different tolerances. It was also noticed that scaling helped in minimizing time by reducing the non-dimensional disparity between the variables and constraints. Also the majority of the dimensions were taken in inches and pounds which helped in reducing the non-dimensional difference between variables, constraints and parameters. The parameters selected for the equations are mentioned below:

Table 10: Parameters and their values.

Parameter	Value
Young's modulus (E)	550000 psi
Poisson ratio (ν)	.1
Yield Stress (σ_y)	3000 psi
Density (ρ)	.0056 Lbf/in^3
Taper Angle	0°
Taper start and end point	.3 and 1
Dihedral Angle	0°
Dihedral start and end point	.5 and 1
Geometric Twist	0°
Wing Span (half wing)	4.75 feet
Cord length of first rib	10 inches
Lift force (whole wing)	20 Lbf
Nr	8
Ns	3

2.2.5 Optimization Study

The optimization study involved using Optimus, Matlab and Abaqus. The overall structure is OPTIMUS à MATLAB à PYTHON à ABAQUS à MATLAB à OPTIMUS. Optimus provides inputs to a Matlab file which contains the variables and the constraints. The Matlab file then generates a Python script and an external batch file is used to run Abaqus which conducts an F.E.A based on values of variables. While the versions of Optimus and Abaqus, unfortunately do not link directly, we identified a method to convert the output from Abaqus into a text file which is read by Matlab. Matlab pulls out the displacements and other outputs from the text file. The overall time for each iteration was over 2 mins. The Optimus structure looks as shown in Appendix A. Over 20 runs have been conducted with variable number of iterations, with some runs over 8 hrs. The initially the model was simplified to 3 variables and was then increased to 6

variables. The parametric study was simplified to reduce run time. Only the important results have been included to minimize length of the report.

The optimization method used a combination of two methods EGO followed by SQP. An intensive EGO run was conducted then the results of which were used as nominal values in SQP. The value from SQP more or less converged with the optimized results from EGO.

Table 11: Results of EGO run.

	Start	End (124)	Low	High
Inputs				
Hs1	0.701259976	1.25	0.25	1.25
Hs2	0.551260018	1.25	0.25	1.25
tr	0.130900967	0.1	0.1	0.75
a2	1.668161276	1.962912376	0	5
Ws1	0.693369028	0.53583017	0.125	0.75
Ws2	0.343623992	0.742665454	0.125	0.75
Outputs				
mass	0.424084	0.764564		
g1	1.38018	-0.072286		0
g2	-3.2434	-9.482		0
g5	-2.99934	-3.001251		0
g6	-2.988417	-2.989691		0
g7	-2.977494	-2.978131		0
g8	-2.966571	-2.966571		0
g10	-2.944726	-2.943451		0
g9	-2.955649	-2.955011		0
g11	-2.933803	-2.931891		0
g3	1.929094	-8.60E-04		0
g4	0.550881	-0.328576		0
GOAL	0.424084	0.764564		

Table 12: Results from SQP.

	Start	End (1.0.0.4)	Low	High
Inputs				
Hs1	1.25	1.25	0.25	1.25
Hs2	1.25	1.25	0.25	1.25
tr	0.1	0.1	0.1	0.75
a2	1.96291	1.96487391	0	5
Ws1	0.533583	0.533583	0.125	0.75
Ws2	0.74267	0.74267	0.125	0.75
Outputs				
mass	0.762773	0.762773		
g1	-0.072083	-0.072054		0
g2	-9.403	-9.425		0
g5	-3.001251	-3.001263		0
g6	-2.989691	-2.989699		0
g7	-2.978131	-2.978135		0
g8	-2.966571	-2.966571		0
g10	-2.943451	-2.943444		0
g9	-2.955011	-2.955008		0
g11	-2.931891	-2.93188		0
g3	1.62E-04	4.50E-05		0
g4	-0.330101	-0.331027		0
GOAL	0.762773	0.762773		

The EGO run allows us to access the kriging meta-model, hence the solution is more or less likely to be a global minimum. Since the EGO run was performed before some of the data was used for the SQP solutions which reduced run time. The upper bound constraint for the Hs1 and Hs2 is active. The upper bound of the spars can be changed in-order to find a more suitable solution. It also shows that the thickness of the ribs is at its minimum. Hence, constraint G13 for tr is active. It can also be seen from the tables that constraints G1 and G3 are more or less active with their values close being close to zero. These are the stress and the displacement constraints. All other constraints can be considered as in-active or possibly active in a region wise sense. The second SQP run with a higher tolerance and greater number of line search steps was conducted to re-check the results. The values were very close to the EGO run. They have been included in Appendix A.

2.2.6 Parametric Studies

Given the length of the project and in order to minimize the run time from 8 hours, the parametric study was conducted by fixing certain variables as constants and bringing the total number of variables down to 3 from 6. Variables Ws1, Ws2 and tr were fixed to the nominal values from the SQP run. After that the following parameters were varied in order to study the change in the objective.

Table 13: Parametric studies conducted.

Parameters	Test1	Test 2	Nominal
Nr	6	10	8
Ns	3	4	3
b (wing length)	3.75’	5.375’	4.75'

As seen from the results (Appendix A) the mass reduced by decreasing the number of ribs to 6. This is an expected result as the model fails from displacement well before buckling. Similarly increasing the number of ribs to 10 resulted in a 5% change in the dimensions of the spars. Hence, this decreased the weight of the wing. In the test 2 of the parametric study, where Ns equals 4, the mass of the wings increased. This can be attributed to the fact that the change in the dimensions for the spars was not enough as the displacement constraint had to be satisfied. The factor of safety in our case has been assumed to be high.

The number of ribs Nr, does not cause a significant change in mass and hence in the optimum solution. In the NS equals 4 resulted in a 33% increase in the optimum mass value from the nominal SQP case. Hence, Ns is very important in determining the wing structures optimum weight. The third parameter varied was the length of the wings. The mass and the optimum increase with increase in length and decrease with reduction of length. This parameter has more bearing in the system optimization as compared to the sub-system optimization because it will increase lift.

2.2.7 Discussion of Results

The results are very much in line with the model. The F.E.A analysis and the optimum prove that in a practical scenario where the loading is provided, the wing will deflect before buckling or shearing. This makes the deflection or displacement constraint very important. The weight of the wings in comparison to the model designed by the M-Fly team should be and is less. This is

because of the variable spacing between the individual ribs in our design gives more structural strength where required and hence preventing constraint G_1 and G_2 from being violated. The M-Fly team had ribs that were equally spaced over the length of the wing. Our model results in reduces the of required number of ribs. Our model does not take into account the weight of the glue and the skin that will go on the wing; additional parameters will be assumed for these values in the system optimization.

The upper dimensional bounds for the Ws1, Ws2, etc. were selected for construction feasibility and minimizing the run time. These can be increased to find a more optimized structure. Also adding additional spars adds more weight than strength. It is possible that reducing the number of spars to two might decrease the optimum further. But, a completely different topology would have to be created in order to test this scenario.

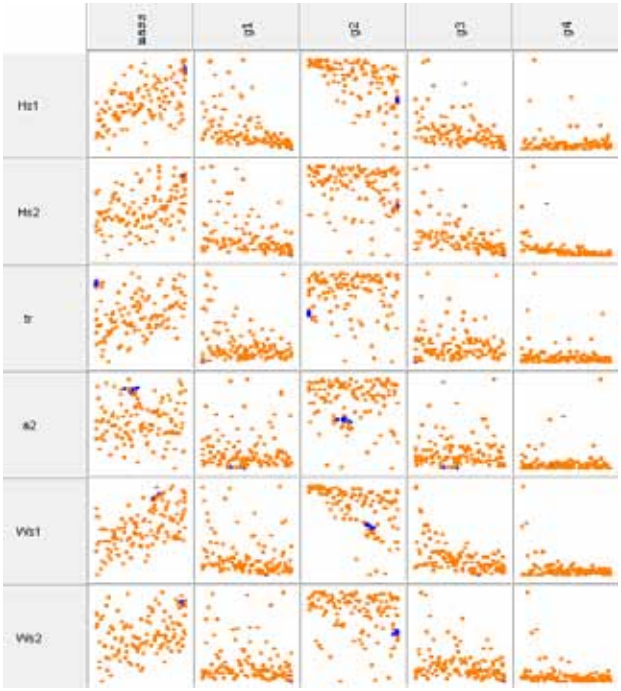

Figure 6: Scatter plot of EGO search -- blue points are near minimal solutions (full-sized image located in Appendix A)

Our optimum solution was an interior point. However as shown in Figure 6 the solution occurred very close to the bounds in all variables. The optimum is also located near the boundary in most of our constraints as well. Only the G_2 constraint shows the minimum far away from the boundary. Figure 6 also supports our statement that $G_1$and G_3 are most likely active but in an heuristic method there is no way to be sure.

2.3 Landing Gear Assembly Subsystem (by Mohit Mehendale)

This sub-section develops the optimization framework for the landing gear assembly, another component that in the past, M-Fly has experienced structural integrity challenges with.

2.3.1 Problem Statement

The landing gear is one of the most critical components of the aircraft, capable of reaching the largest local loads on the airplane. It is a primary source of shock attenuation at landing. The landing gear would be subjected to both static and dynamic loads.

The primary objective of the design optimization problem is to minimize the weight of the landing gear and be able to withstand the static and dynamic forces the aircraft is subjected to before take-off, during take-off and upon landing (impact). This is because during landing and take-off, the landing gear assembly must absorb huge amounts of energy without generating reaction forces that exceed the dynamic loads envelope.

The desired characteristics of a landing gear are high strength, lightweight, medium stiffness and high elastic strain energy storage capacity. A tradeoff occurs, since we have to maximize the load carrying capacity without the weight of the landing gear to be high (because of the weight-minimization objective). Also, the strength, stiffness etc. would depend on the weight and design.

The latest design of the M FLY team is as shown in Figure 7 that follows.

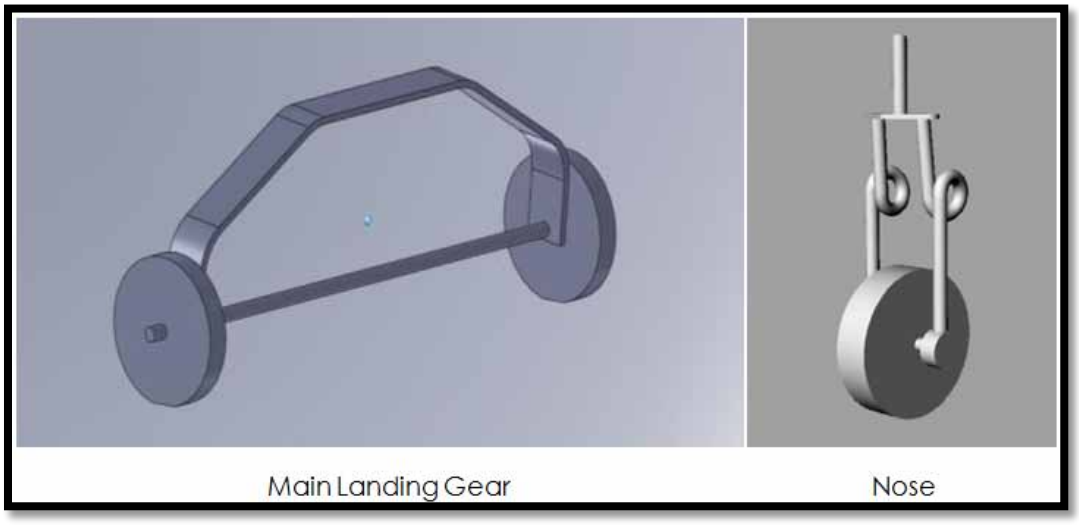

Figure 7: Feasible landing gear design without optimization.

This design was not optimized and hence the weight of the landing gear is high. This serves as a motivation for the present design optimization problem to in order to minimize the weight of the landing gear.

A standard solid spring design was chosen for the landing gear, as shown in the figure below.

2.3.2 Nomenclature

d_w: Wheel Diameter

t_w: Wheel thickness

h1: Height of airplane above the landing gear

h2 : height of the landing gear

w_p: width of the main landing gear plate

l_p : Length of plate

t_p: Thickness of plate

σ: Stress

σ_{yield} : Yield Strength

g : Acceleration due to gravity

S.F. : Factor of Safety (Assumed to be 2.5)

Θ : Angle of the solid spring with the vertical as shown in figure (assumed to be 60 deg)

η : Efficiency of the shock absorber (assumed to be 0.5 for solid spring)

L_{avg} : Average load acting on the shock absorber (solid spring)

S : Stroke (Total deflection of the solid spring)

F : Force acting on the shock absorber

W_{AC} : Weight of the aircraft acting on the landing gear = $W_s + W_p + W_F$

L_{AC} **:** Length of the aircraft

Subscript ‘n’ denotes the values for the nose of the landing gear.

For the landing gear, the solid spring type of design is chosen in a tricycle configuration as shown in the figure on the next page.

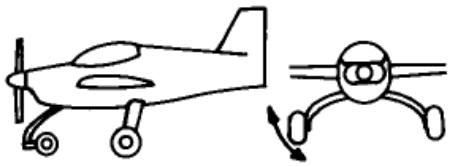

SOLID SPRING

Figure 8: Solid Spring Design for landing gear

2.3.3 Mathematical Model

This sub-section presents the scientific relations between the parameters and variables to be used in the optimization process.

2.3.3.1 Objective Function

The objective function is to minimize the weight of the landing gear.

The implicit analytical expression of the objective is:

$$\text{Min.} \quad W_{LG} = \text{fn}(d_w, t_w, w_p, l_p, t_p)$$

Using the Volume and density to find the weight of the landing gear we get:

$$\text{WLG} = [\ \{(\pi)(\text{dw}/2)2(\text{tw})\} + (\text{wplptp})] * \rho\text{Al} * g$$

General stress constraint in order to define structural integrity: σ_{yield} should be greater than stresses induced during static and dynamic (landing) loadings:

$$\sigma \leq \sigma_{yield} / \text{S.F}$$

$$\sigma = \text{fn}\ (d_w, t_w, w_p, l_p, t_p)$$

The equation is :-

$$F\ l_p / (\ w_p\ \ t_p^3) / (\ t_p/2) - \sigma_{yield} / \text{S.F} \leq 0$$

Which further reduces to

$$6F\ l_p / (\ w_p\ \ t_p^2) - \sigma_{yield} / \text{S.F} \leq 0$$

Substituting (for analysis) the value of the force we get:-

$$2.7 W_{AC} l_p / w_p t_p^2 + 2.7 * \rho_{Al} * g * (\ l_p^2 / t_p\ +\ (\pi/4) * (d_w^2 t_w l_p / w_p / t_p^2)) - 3199.444 \leq 0$$

The dimensional restrictions are ≤ 225 inches

Therefore the equation becomes:-

$$L+B+(h_1+h_2) -225 \leq 0$$

In terms of the height of the landing gear h_2, the equation reduces to

$$l_p \cos \Theta + (d_w \cos 30)/2 + (L_{AC} + b + h_1 - 225) \leq 0$$

Deflection (stroke) constraint

Vertical Energy of the aircraft must be absorbed during landing

$$\text{K.E. (vertical)} = (1/2) * (W_{AC}/g) * v^2$$

Also, energy absorbed by deflection

$$\text{K.E. (absorbed)} = \eta * L_{avg} * S$$

Therefore

$$S = V^2/(2g \eta N_{gear})$$

Also, the deflection can be found out by using the beam equations:-

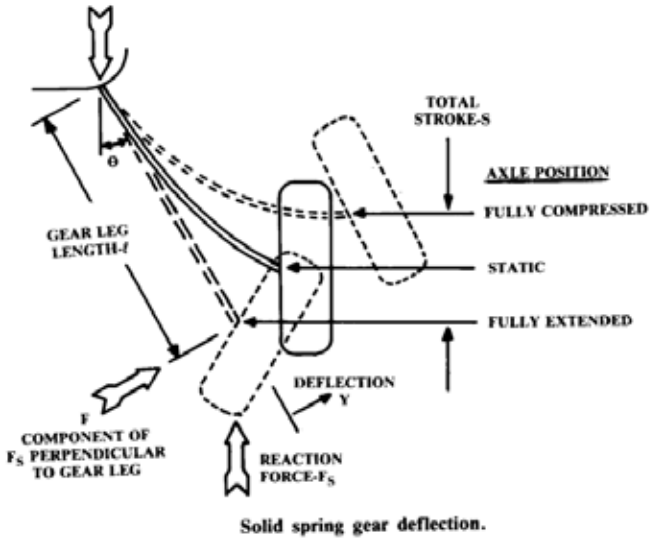

Figure 7: Deflection geometry

$$S = (W N_{gear}/2) \sin^2\Theta \, l_p^3 /3EI$$

Equating the two stroke equations we get

$$(4 N_{gear}^2 g \eta / v^2 E) (W_T \sin^2\Theta \, l_p^3 w_p t_p^3) -1=0$$

Substituting the value of W_T *we get the following equation*

$$(4 N_{gear}^2 g \eta / v^2 E)[W_{AC} + (\{(\pi)(d_w/2)^2(t_w)\} + (w_p l_p t_p)) * \rho_{Al} * g] \sin^2\Theta \, l_p^3 w_p t_p^3) -1=0$$

Upper and Lower bounds need to be set for the problem to ensure that feasible values are obtained. These bounds are set based on the previous designs and manufacturability limits.

The bounds set on the variables are as follows (all dimensional values are in metres, agles in radians) :-

$0.254 \leq l_p \leq 0.6$

$0.025 \leq w_p \leq 0.11$

$0.007 \leq t_p \leq 0.055$

$0.05 \leq d_w \leq 0.5$

$0.0127 \leq t_w \leq 0.05$

$0.1745 \leq \Theta \leq 1.0472$

Both the landing gear components, the main landing gear and the nose are similar to each other, the difference being the placement of the wheel.

2.3.3.2 Summary Model

For Main landing gear

Min. $W_{LG} = [\ \{(\pi)(d_w/2)^2(t_w)\} + (w_p l_p t_p)] * \rho_{Al} * g$

s.t. $g1 : 6F\ l_p / (\ w_p\ t_p^2) - \sigma_{yield} / \text{S.F} \leq 0$

$g\ 2 : l_p \cos\Theta + (d_w \cos 30)/2 + (L_{AC} + b + h_1 - 225) \leq 0$

$h\ 1 : (4\ N_{gear}^2\ g\ \eta / v^2 E)\ (W_T \sin^2\Theta\ l_p^3\ w_p t_p^3) - 1 = 0$

For Nose

Min. $W_{LGnose} = [\ \{(\pi)(d_{wn}/2)^2(t_{wn})\} + (w_{pn} l_{pn} t_{pn})] * \rho_{Al} * g$

s.t. $g1 : 6F\ l_p / (\ w_p\ t_p^2) - \sigma_{yield} / \text{S.F} \leq 0$

$g\ 2 : l_p \cos\Theta + (d_w)/2 + (L_{AC} + b + h_1 - 225) \leq 0$

$h\ 1 : (4\ N_{gear}^2\ g\ \eta / v^2 E)\ (W_T \sin^2\Theta\ l_p^3\ w_p t_p^3) - 1 = 0$

For both components of the landing gear, the following bounds have been set.

$0.254 \leq l_p \leq 0.6$

$0.025 \leq w_p \leq 0.11$

$0.007 \leq t_p \leq 0.055$

$0.05 \leq d_w \leq 0.5$

$0.0127 \leq t_w \leq 0.05$

$0.1745 \leq \Theta \leq 1.0472$

Initially a model in Abaqus was created for carrying out the optimization using Optimus, but the simulation could not be run due to version differences. These problems were resolved at a later stage and has been used in the structures subsystem, but due to the time constraint, it could not be applied to this subsystem.

The constraint equations were found out manually by assuming the beam structure, not by FEA-Optimus linking (because of the software problems).

2.3.4 Model Analysis

Table 14: Monotonicity table for landing gear structure.

	l_p	w_p	t_p	d_w	t_w
W	+	+	+	+	+
g1	+			+	+
g2	+			+	
h1	+	+	+	+	+

By analyzing the model, it can be seen that the equality constraint, h1 can be set as active with respect to the variables or it can be directed to eliminate variables from the problem statement.
From the results obtained in MATLAB, it is seen that at the optimum values the weight of the landing gear is reduced significantly. This is because at the starting feasible point, all the constraints are satisfied but the weight is high. The dimensions of the landing gear are optimized in such a way that the stress and deflection constraints remain valid along with the dimensional constraints. It is important that the yield stress value with the factor of safety is not exceeded, which is possible by redistributing the dimensions within the model.The maximum stress is expected at the joint of the landing gear to the aircraft.

2.3.5 Optimization Study

The optimization was carried out using MATLAB with the function *fmincon*. The solution obtained is a local solution. The monotonicity analysis observations agree with the results obtained. As expected from the analysis, the deflection constraint h1 is active.

The solution changes with change in starting points. For different starting points in particular ranges, a different solution is obtained.

The problem above was solved using MATLAB function *fmincon*.

The values obtained are (MAIN LANDING GEAR):
l_p=0.3382 m
w_p=0.0398 m

t_p=0.0076 m

d_w=0.0500 m

t_w=0.0127 m

Θ=0.3486 rad (20 degrees)

The original Function Value was 5.4866N, for the starting point (l_p=0.47 w_p=0.050 t_p=0.00635 d_w=0.0762 t_w=0.0127 Angle Θ= 0.5236 rad) which after optimization was reduced to 3.3581 N.

The values obtained are (NOSE):
l_p= 0.3462 m
w_p= 0.0262 m

t_p= 0.0049 m

d_w= 0.0479 m

t_w= 0.0106 m

Θ= 0.1745 rad (10 degrees)

The original Function Value was 5.4025 N, for the starting point (l_p=0.46 w_p=0.050 t_p=0.00635 d_w=0.0762 t_w=0.0127 Angle Θ= 0.5236 rad) which after optimization was reduced to 1.6892 N.

Weight= 2*(3.3581) + (1.6892) = 8.4054 N

Hence, the total weight after optimization of the design for the whole landing gear subsystem = 8.4054 N.

2.3.6 Parametric Study

Different solutions were obtained for different sets of parameter values. The optimum changes with the change in the parametric values. This is because the stress and stroke (deflection) values change which results in a change in the optimum. The results obtained can be generalized to a particular range of the parameter values of weight, landing velocity etc.

2.3.7 Discussion of Results

The results obtained are practically feasible and appear to make sense. The model limits the solution in terms of the manufacturability of the landing gear within some ranges. Practical constraints would be the non-proportional dimensional values obtained for the different ranges if values. Some of the results obtained are not practical which is due to the limitation of the model. For e.g a very small wheel or plate thickness but higher plate length and width. This would imply that more constraints can be introduced in the subsystem based on the practical constraints.

To make the problem interesting and to attempt to improve the answer, a possible idea would be to analyze the model in FEA softwares like Abaqus etc. and optimize the results with the help of softwares like Optimus, iSight etc.

3 System

For the system analysis we combined our subsystems as shown in figure#9. The constraints and variables used are exactly the same as the subsystems. The individual subsystems were modeled such that parameters in one subsystem were variables in other and vice-versa.

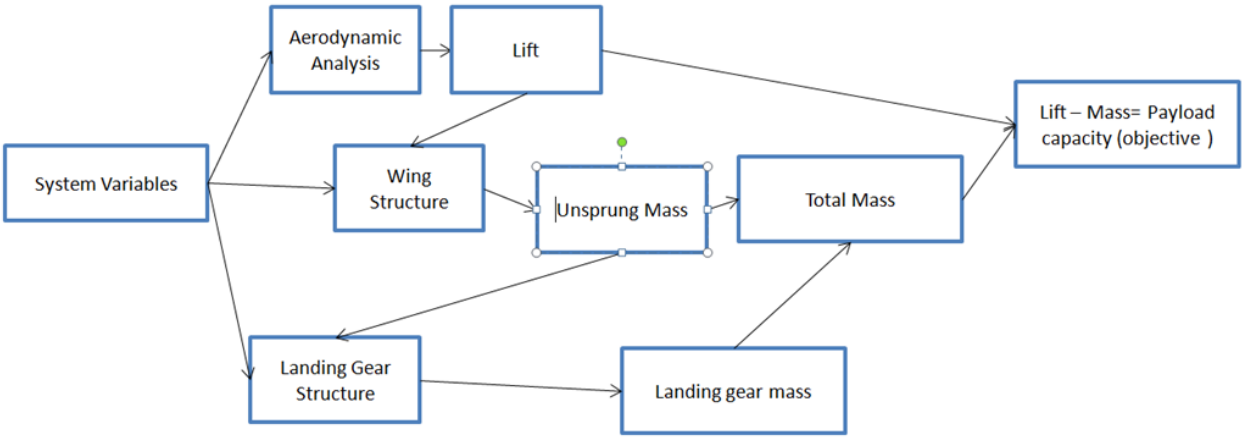

Figure 9: Flow of how the system integration study will work.

Our system was broken up by discipline but also by component. The wing component was broken into two disciplines: Aerodynamics and Structure. The second component is the Landing Gear. During the subsystem optimization we observed that the landing gear structure and wing structure analysis had parameters that were outputs from other system. The mass from the wing and the landing gear were used as parameters for the aerodynamic solver and the lift was a parameter in the wing structure. This complicated the optimization as the mass (output from structure) needed to proceed with the aerodynamic routine and the lift (output from aerodynamics) was needed to proceed with the structure run. Conducting an absolute All-in-one (AIO) approach would create a loop scenario for these variables. This was avoided by partially decomposing the system and first evaluating the mass from the dimensions specified by the aerodynamics, which was fed into the solver to generate the lift. The lift was finally used evaluate the stresses and hence check the structural integrity of the air-plane. This resulted in a significant increase in the computation time for the entire model.

The system model had 18 variables and 24 constraints with the objective remaining the same as before which was to maximize the payload. Some of the variables were assumed as parameters in order to minimize computation time. These assumptions were made based on significance to the objective e.g. the landing gear variables had a very small contribution to the weight and the lift of the aircraft. The system design problem statement is as follows:

Objective:

$minimize - Wp = \ W_T - L$

Where W_T includes the weight of the engine, radio, servos, and etc.

Variables:

Ws1= width of front spar(s) (V)

Ws2= width of rear spar(s) (V)

H_{s1}= height of front spar(s) (V)

H_{s2}= height of rear spar(s) (V)

a2= Quadratic spacing between ribs (V)

t_r= thickness of ribs (V)

b_w = wing span (V)

C_W = wing chord length (V)

$X_{w =}$ distance from nose to wing leading edge

b_h = span of horizontal tail

b_v = span of vertical tail

C_V = vertical tail chord length (V)

C_h = horizontal tail chord length (V)

X_h = distance from nose to horizontal tail

X_v = distance from nose to vertical tail

f_{ail} = fraction of wingspan used for ailerons

f_{rud} = fraction of vertical tail span used for rudder

f_{ele} = fraction of horizontal tail span used for elevator

Constraints:

Constraints G_1 to G_{12} are same as the structures subsystem on page 17-20. Constraints G_{13} to G_{25} are the constraints as listed in the Aerodynamics subsection. The rest of the constraints on the structure subsystem have been implemented as upper/lower bounds directly in Optimus and have not been mentioned here as they are purely dimensional in nature and have been selected based on materials available and reduction of optimization time.

In order to optimize the system we used Optimus and conducted an EGO run for the entire system followed by SQP. More than five EGO and SQP runs were conducted on the system. Based on the initial EGO runs it was noticed that some of the variables in the system optimization were extremely sensitive to variation, for example the wing chord length. The bounds of these variables were changed accordingly in order to obtain a feasible space. The other alternative would have been to modify the Abaqus F.E.A file which would take more time than the project time frame would allow.

After the first few nominal EGO runs, the wing chord length had to be further constrained from above (i.e. lower the upper bound) due to the set-up of the wing structure. The existing Abaqus model for the wing structure was unable to bear loads (without adding another spar to the model) if the wing chord length went beyond 30cm. After reducing the upper bound on the chord length variable, EGO could proceed smoothly with minimal effect on the optimal result. This was because the new upper bound value for the chord length was set based on the optimal results from the Aerodynamics subsystem.

The first few EGO runs violated constrains as the number of experiments and iterations were not large enough. The SQP runs converged to a similar value within 5% of the last run and hence the optimum that was attained could be a global minimum.

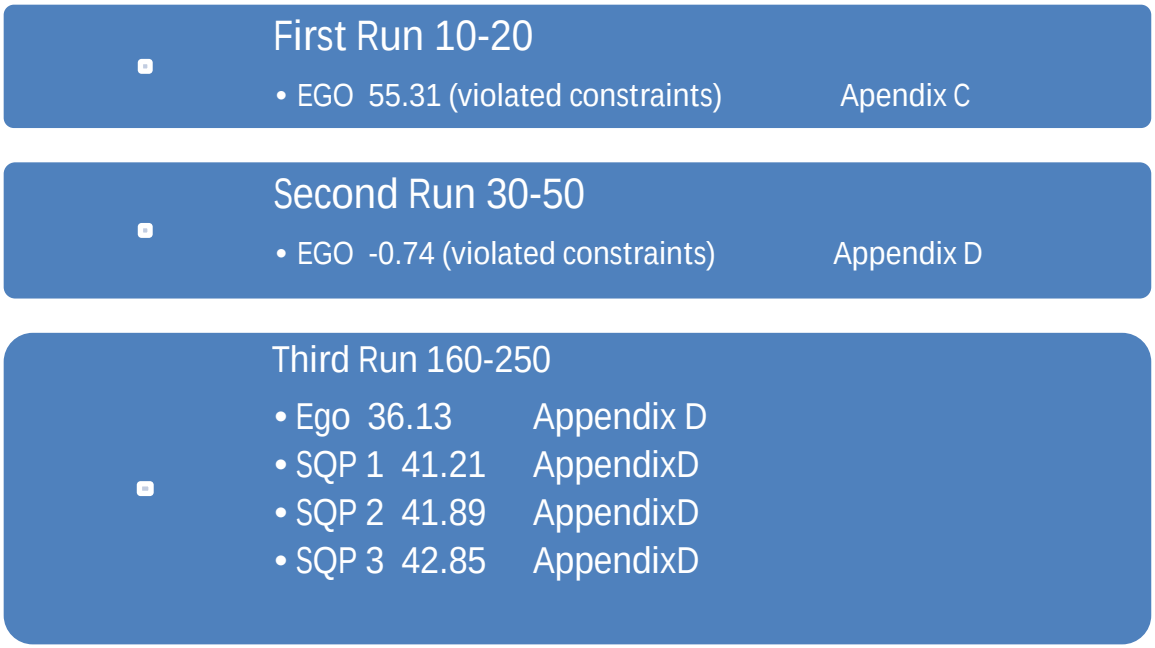

4 Acknowledgements

We would like to thank the Michigan M-Fly team for providing us with the initial data and the background on the project. The initial data for plane structure, shape and components for the plane along with the project idea was arrived at from the M-fly team's past designs and the SAE Aero design competition rules.

5 References

[1] Nicholai, L.M., "Estimating R/C Model Aerodynamics and Performance", Technical Fellow, Lockheed Martin Aeronautical Company, 2009.

[2] Raymer, D.P., "Aircraft Design: A Conceptual Approach", 4th Edition, AIAA, 2006.

[3] Moiseev, D. "Course Notes for ME 204 Mechanical Design", University of Rochester, 2009.

Appendix A: Aerodynamics MATLAB Scripts & EGO Set-Up

```
%% Optimizer (main script)

%% Parameters
load('param.mat');
%% Starting Point
%     bW  cW  xW  bH  bv    cH   cV   xH    xV  bAil% bRud% bEle%
x0 = [1.0 0.4 0.6 1.6 0.51 0.35 0.223 1.78 1.907 0.8 0.8 0.7]';

%% Function Evaluations
% run AVL case #1 to get Xcg & Xnp & eigv --> nonlcon.m
% run AVL case #2 to get CD_red & CL_red --> TOcalc.m
% run AVL case #3 to get CL(t), CL1 --> func.m

A = [1 0 0 0 1 0 0 0 0 0 0 0; % 3-dimensions
     0 0 0 0 0 1 0 1 0 0 0 0; % limit htail to max. length of fuselage
     0 0 0 0 0 0 1 0 1 0 0 0]; % limit vtail to max. length of fuselage
% b = [dim_lim-LG_ht-fuse_rad-fuse_length; 0; 0; 0; fuse_length; fuse_length];
b = [dim_lim-LG_ht-fuse_rad-fuse_length; fuse_length; fuse_length];
Aeq=[]; % no equality constraints
beq=[];
lb=[1 .1 .1 .4 .2 .1 .1 .3 .3 .1 .1 .1]'; % all geometries must be >1cm
ub=[10 3 fuse_length 2 2 1 1 fuse_length fuse_length 1 1 1]';
options = optimset('DiffMinChange',0.001,'TolFun',1e-2);
[x_opt Lift_max] = fmincon('func',x0,A,b,Aeq,beq,lb,ub,'nonlcon',options)
nonlcon(x_opt)
disp('Meets 3D constraints?');
(A(1,:)*x_opt)<b(1)
A(1,:)*x_opt + LG_ht+fuse_rad+fuse_length
```

```
%% Objective Function Calculator
function L=func(x)
load('param.mat'); % parameters (rho)

[Xcg, Xnp, CL_rolloff, CD_rolloff, CL_TO, CL_root_TO, eig_real_1, eig_real_2,
eig_real_3]=test_main(x);
[SG V_TO]=TOcalc(x,CL_rolloff,CL_rolloff); % V_TO
S=x(1)*x(2);
L = -0.5*rho*V_TO^2*S*CL_TO
end
```

```
%% Non-Linear Constraint Calculator
function [c, ceq]=nonlcon(x)

load('param.mat'); % parameters
[Xcg, Xnp, CL_rolloff, CD_rolloff, CL_TO, CL_root_TO, eig_real_1, eig_real_2,
eig_real_3]=test_main(x);

[SG V_TO]=TOcalc(x,CL_rolloff,CD_rolloff);
c1=SG-SG_lim; % take-off distance limit

S=x(1)*x(2);
```

```
L = -0.5*rho*V_TO^2*S*CL_TO
c2=W+L; % (W-L)

c3=CL_root_TO-CLmax; % CL1= wing root CL (highest)

c4=SM_lim-(Xnp-Xcg)/fuse_length; % static margin

c5=eig_real_1-0.24; % some buffer for Short Period (slow settling time)

c=[c1 c2 c3 c4 c5']';
ceq=[];

end
```

```
%% Complete run
function [Xcg, Xnp, CL_rolloff, CD_rolloff, CL_TO, CL_root_TO, eig_real_1,
eig_real_2, eig_real_3]=test_main(x)

%% One: try to change variables
 load('m3b_inp_ftest.mat')

%test changing a value
b_wing = x(1);
c_wing = x(2);
x_wing = x(3);
b_htail = x(4);
b_vtail = x(5);
c_htail = x(6);
c_vtail = x(7);
x_htail = x(8);
x_vtail = x(9);
b_ail = x(10)*(b_wing/2-0.2);
b_rud = x(11)*(b_vtail-0.08);
b_ele = x(12)*(b_htail/2-0.1);

% x = [b_wing; c_wing; x_wing; ...
%     b_htail; b_vtail; c_htail; ...
%     c_vtail; x_htail; x_vtail;...
%     b_ail; b_rud; b_ele];

%
save('m3b_inp_ftest.mat', 'b_wing', 'c_wing', 'x_wing', 'b_htail', 'b_vtail',
'c_htail', ...
    'c_vtail', 'x_htail', 'x_vtail', 'b_ail', 'b_rud', 'b_ele');

%% Two: test generation of mass and avl file
m3b_mass_gen('m3b_ftest.mass', 'm3b_inp_ftest.mat')
m3b_avl_gen('m3b_ftest.avl', 'm3b_inp_ftest.mat')
m3b_run_gen('m3b_ftest.run')

%% Three: run avl
avl_dir = 'C:\Users\WoW\Documents\2011W\ME555\Project ';
avl_file = 'm3b_ftest.avl ';
```

```
input_file = 'avl_cmd.txt';
st_file1 =  'st1_ftest.txt';
run_file1 = 'run1_ftest.txt';
ft_file2 = 'ft2_ftest.txt';
fs_file3 = 'fs3_ftest.txt';
ft_file3 = 'ft3_ftest.txt';
eig_file = 'eig_ftest.txt';

run_avl(avl_dir, avl_file, input_file, st_file1, run_file1, ft_file2,
fs_file3, ft_file3, eig_file)

%% Four: Extract outputs
[Xcg, Xnp, CL_rolloff, CD_rolloff, CL_TO, CL_root_TO, eig_real_1, eig_real_2,
eig_real_3]= m3b_readout(st_file1, run_file1, ft_file2, fs_file3, ft_file3,
eig_file);
```

```
%% Take-off Distance Calculator
function [SG V_TO]=TOcalc(x,CL_rolloff,CD_rolloff)

load('param.mat'); % parameters
S= x(1)*x(2);

% unit conversions
NtoP=.224808943; % 1 N to pounds-force
MStoFTS= 3.2808399; % 1m/s to 1ft./s
FtoM= 0.3048; % 1 ft. to m

V_TO = sqrt(2*W/(S*rho*0.8*CLmax)); % desired/required take-off velocity

% using 0.7*V_TO, everything in [POUNDS]
T_red = -2.698*1e-4*(0.7*V_TO)^2 - 4.908*1e-2*(0.7*V_TO) + 7.1; % engine
tests
%CD_rolloff = 0.06895; % ran in AVL for 0.7*V_TO initial.run case #1
D = NtoP*(0.5*rho*(0.7*V_TO)^2*S*CD_rolloff);
%CL_rolloff = 0.9666; % ran in AVL for 0.7*V_TO initial.run case #1
L_red = NtoP*(0.5*rho*(0.7*V_TO)^2*S*CL_rolloff);
a_mean = 32.2/(W*NtoP)*((T_red-D)-0.03*(W*NtoP-L_red));

% output
SG = FtoM*((MStoFTS*V_TO)^2/(2*a_mean)); % runway distance required for take-
off
End
```

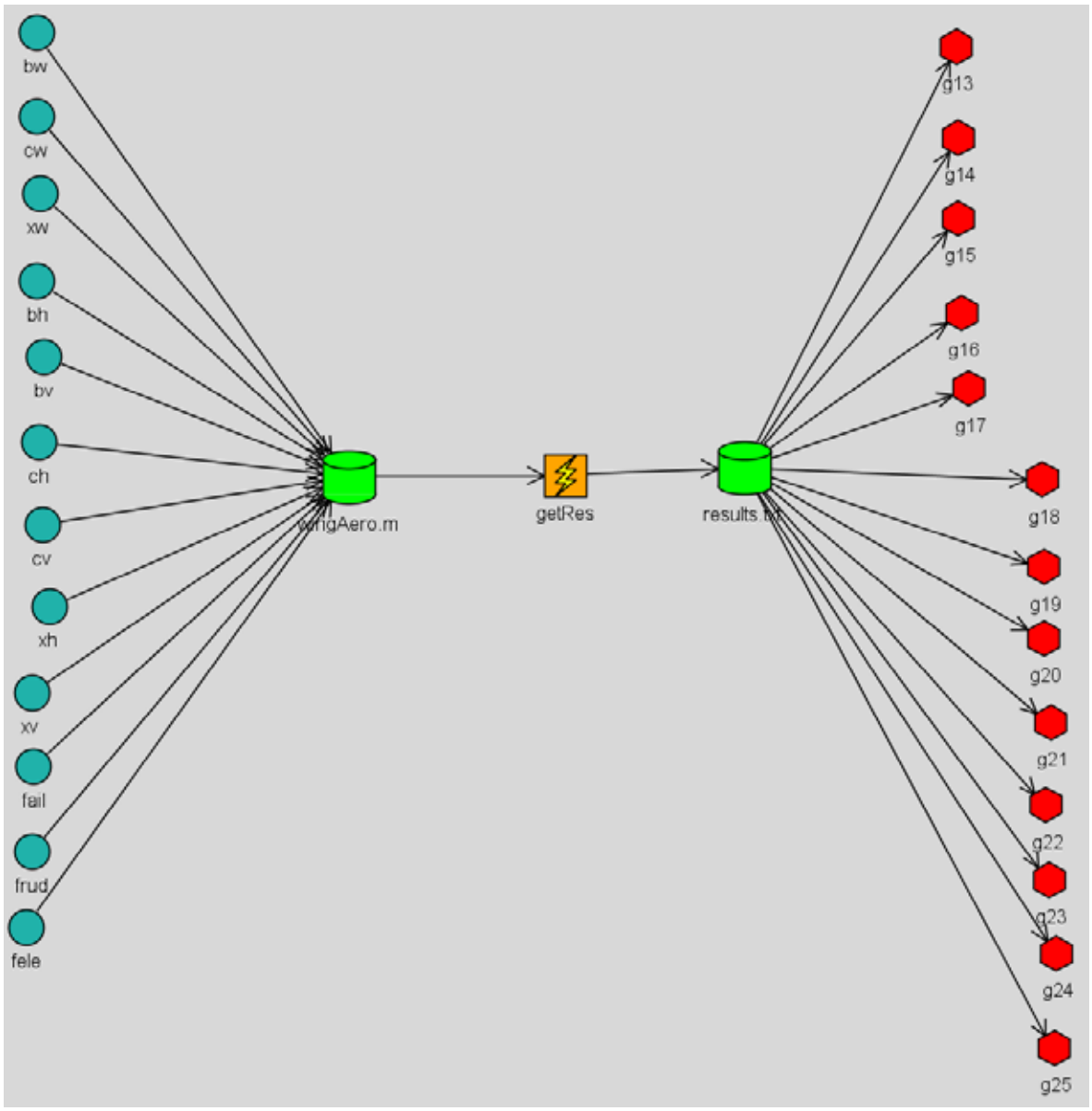
bw
cw
xw
bh
bv
ch
cv
xh
xv
fail
frud
fele
getRes
g13
g14
g15
g16
g17
g18
g19
g20
g21
g22
g23
g24
g25

Appendix B: Structures Subsystem Results

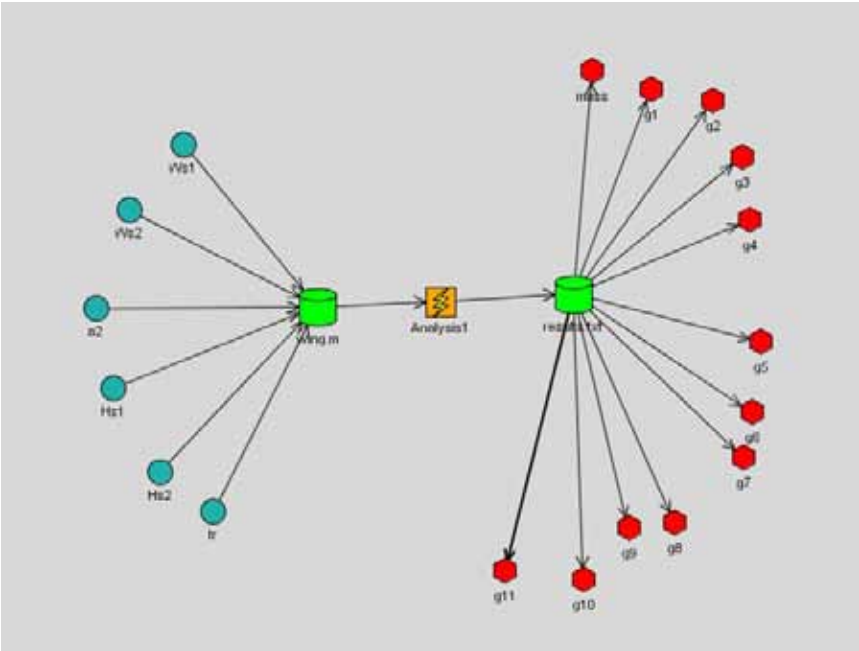

b=5.375'	**Start**	**End (33)**	**Low**	**High**
Inputs				
Hs1	0.379645837	1.25	0.25	1.25
Hs2	0.474309532	1.22333773	0.25	1.25
a2	2.424446108	5	0	5
Outputs				
mass	0.436292	0.972906		
g1	0.451806	-0.055837		0
g2	0.2172	-18.429		0
g5	-2.99785	-3.006542		0
g6	-2.983853	-2.989647		0
g7	-2.969855	-2.972752		0
g8	-2.955857	-2.955857		0
g10	-2.927862	-2.922067		0
g9	-2.941859	-2.938962		0
g11	-2.913864	-2.905173		0
g3	2.474691	0.145897		0
g4	0.369507	-0.411536		0
GOAL	0.436292	0.972906		

SQP	**Start**	**End (1.0.0.6)**	**Low**	**High**
Inputs				
Hs1	1.25	1.25	0.25	1.25
Hs2	1.25	1.25	0.25	1.25
tr	0.1	0.1	0.1	0.75
a2	1.96291	1.96291	0	5
Ws1	0.533583	0.533583	0.125	0.75
Ws2	0.74267	0.74341367	0.125	0.75
Outputs				
mass	0.762773	0.76307		
g1	-0.072083	-0.072173		0
g2	-9.403	-9.435		0
g5	-3.001251	-3.001251		0
g6	-2.989691	-2.989691		0
g7	-2.978131	-2.978131		0
g8	-2.966571	-2.966571		0
g10	-2.943451	-2.943451		0
g9	-2.955011	-2.955011		0
g11	-2.931891	-2.931891		0
g3	1.62E-04	-9.50E-05		0
g4	-0.330101	-0.330509		0
GOAL	0.762773	0.76307		

Nr=6	**Start**	**End (28)**	**Low**	**High**		***Nr=10***	**Start**	**End (31)**	**Low**	**High**
Inputs						**Inputs**				
Hs1	0.748915872	1.25	0.25	1.25		Hs1	0.379645837	1.25	0.25	1.25
Hs2	0.78109885	1.24976263	0.25	1.25		Hs2	0.474309532	1.193187241	0.25	1.25
a2	3.374056118	2.95403089	0	5		a2	2.424446108	5	0	5
Outputs						Outputs				
mass	0.468626	0.749133				mass	0.292684	0.759747		
g1	1.4552	-0.070625		0		g1	3.54031	-0.069425		0
g2	-4.0527	-8.804		0		g2	-0.3041	-9.489		0
g5	-2.987258	-2.985374		0		g5	-3.014599	-3.020794		0
g6	-2.960629	-2.959687		0		g6	-3.007116	-3.011762		0
g7	-2.934	-2.934		0		g7	-2.999633	-3.002731		0
g8	-2.907371	-2.908313		0		g8	-2.99215	-2.993699		0
g10	-1	-1		0		g10	-2.977184	-2.975635		0
g9	-2.880742	-2.882626		0		g9	-2.984667	-2.984667		0
g11	-1	-1		0		g11	-2.9697	-2.966603		0
g3	1.478984	0.00635		0		g3	4.30768	0.032331		0
g4	-0.22739	-0.298888		0		g4	0.681201	-0.30132		0
GOAL	0.468626	0.749133				GOAL	0.292684	0.759747		
Ns=4	**Start**	**End (33)**	**Low**	**High**		***b=3.75'***	**Start**	**End (46)**	**Low**	**High**
Inputs						**Inputs**				
Hs1	0.379645837	1.25	0.25	1.25		Hs1	0.379645837	1.142910119	0.25	1.25
Hs2	0.474309532	1.12903385	0.25	1.25		Hs2	0.474309532	1.103270609	0.25	1.25
a2	2.424446108	4.66738529	0	5		a2	2.424446108	0.606702772	0	5
Outputs						Outputs				
mass	0.395127	1.00245				mass	0.231601	0.55469		
g1	4.14757	-0.064468		0		g1	2.9437	-0.073929		0
g2	0.2874	-8.753		0		g2	-1.1019	-13.683		0
g5	-3.003682	-3.010684		0		g5	-3.013012	-3.000164		0
g6	-2.991312	-2.99598		0		g6	-3.003246	-2.994681		0
g7	-2.978942	-2.981276		0		g7	-2.99348	-2.989198		0
g8	-2.966571	-2.966571		0		g8	-2.983714	-2.983714		0
g10	-2.941831	-2.937163		0		g10	-2.964183	-2.972748		0
g9	-2.954201	-2.951867		0		g9	-2.973948	-2.978231		0
g11	-2.929461	-2.922459		0		g11	-2.954417	-2.967265		0
g3	4.681695	0.080576		0		g3	3.2365	-0.065672		0
g4	0.616021	-0.179241		0		g4	0.352521	-0.30963		0
GOAL	0.395127	1.00245				GOAL	0.231601	0.55469		

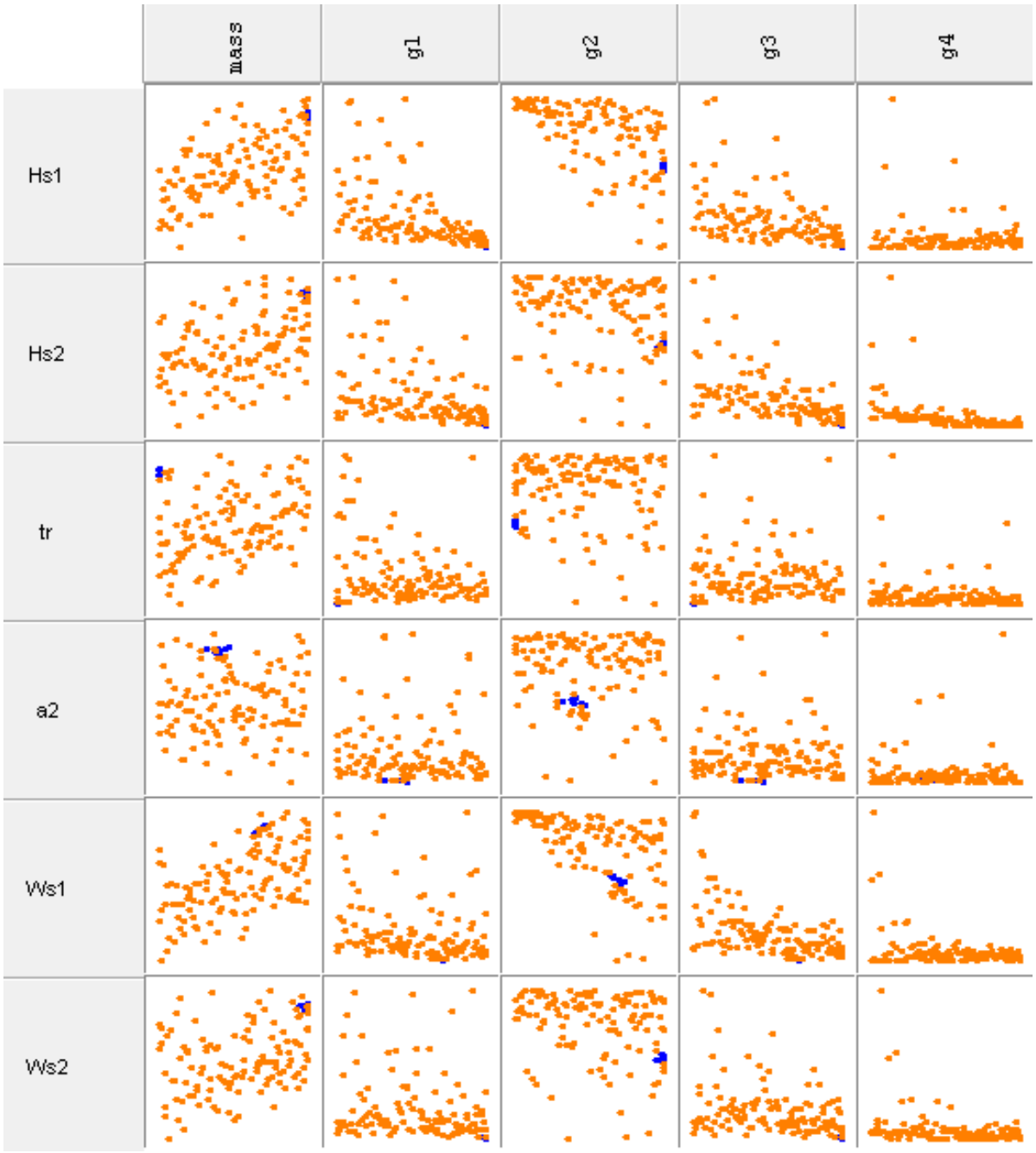

Figure A10: Full-sized version of Figure 3.

Appendix C: System Level Results

SQP 1	Start	End (3.0.0.15)	Low	High	
Inputs					
Hs2	0.5	0.5	0.5	1.5	
tr	0.35	0.35	0.1	0.35	
a2	0.295748	0.247628649	0	5	
Ws1	0.978604	1.053182214	0.5	1.5	
Ws2	0.5	0.52399299	0.5	1.5	
bw	2.394262	2.394262	1	4.5	
cw	0.2676208	0.236027607	0.2159	0.2921	
xw	0.757121	0.807097677	0.1	1.5	
bh	0.5	0.5	0.5	2	
bv	1	1	0.2	1	
ch	0.3319404	0.307875618	0.1	0.6	
cv	0.05	0.050046742	0.05	0.6	
xh	1.733631	1.733631	1.5	2.13	
xv	1.50589	1.50589	1.5	2.13	
fail	0.9	0.900901	0.1	0.9	
frud	0.9	0.9	0.1	0.9	
fele	0.9	0.899563382	0.1	0.9	
Hs1	1.492658	1.5	0.5	1.5	
Outputs					
g1	-545.164282	-272.868903		0	
g2	-1.457148	-1.63953		0	
g5	-0.710214	-0.698711		0	
g6	-0.681827	-0.673611		0	
g7	-0.653441	-0.648511		0	
g8	-0.625054	-0.623411		0	
g10	-0.568281	-0.573211		0	
g9	-0.596667	-0.598311		0	
g11	-0.539894	-0.54811		0	
g3	-0.04502	-0.072143		0	
g4	-0.506187	-0.507786		0	
g12	-0.511507	-0.52301		0	
g13	-0.137698	-0.137698		0	
g14	-8.795312	-1.139477		0	
g17	-0.042255	-0.063571		0	
g20	-0.279704	-0.280055		0	
g22	-2.137206	-2.123231		0	
g15	-36.138763	-41.213559		0	
g18	-3.525175	-3.385685		0	

g23	-0.014729	-0.010029		0	
g16	-0.0378	-0.025		0	
g19	-0.279704	-0.280055		0	
g24	-0.042041	-0.11031		0	
g25	-0.18115	-0.11031		0	
GOAL	-36.138763	-41.213559			

g21	-2.137206	-2.123231		0	

Appendix D: System Level Results 2

SQP 2	Start	End (5.0.0.7)	Low	High	
Inputs					
Hs2	0.95147	0.95147	0.5	1.5	
tr	0.305936	0.305936	0.1	0.35	
a2	1.66839	1.668068901	0	5	
Ws1	0.978604	0.960134931	0.5	1.5	
Ws2	0.5	0.5	0.5	1.5	
bw	2.39426	2.39426	1	4.5	
cw	0.2676208	0.23091099	0.2159	0.2921	
xw	0.7571213	0.684573114	0.1	1.5	
bh	0.5	0.5	0.5	2	
bv	1	1	0.2	1	
ch	0.3319404	0.282618569	0.1	0.6	
cv	0.05	0.05	0.05	0.6	
xh	1.733631	1.733631	1.5	2.13	
xv	1.505892	1.505892	1.5	2.13	
fail	0.9	0.9	0.1	0.9	
frud	0.9	0.9	0.1	0.9	
fele	0.9	0.883743315	0.1	0.9	
Hs1	1.492658	1.429121226	0.5	1.5	
Outputs					
g1	-735.278264	-676.101393		0	
g2	-1.562095	-1.45697		0	
g5	-0.852893	-0.852877		0	
g6	-0.783741	-0.783729		0	
g7	-0.714589	-0.714582		0	
g8	-0.645437	-0.645435		0	
g10	-0.507133	-0.50714		0	
g9	-0.576285	-0.576288		0	
g11	-0.437981	-0.437993		0	
g3	-0.114146	-0.086465		0	
g4	-0.510539	-0.514134		0	
g12	-0.368829	-0.368846		0	
g13	-0.1377	-0.1377		0	
g14	-8.054504	-0.020375		0	
g17	-0.042255	-0.009467		0	
g20	-0.279703	-0.275741		0	
g22	-2.137206	-1.811886		0	
g15	-36.364819	-41.896409		0	

g23	-0.01473	-0.014319		0
g16	-0.0378	-0.0234		0
g19	-0.279703	-0.275741		0
g24	-0.04204	-0.120621		0
g25	-0.18115	-0.120621		0
GOAL	-36.364819	-41.896409		

g18	-3.525168	-3.361732		0	
g21	-2.137206	-1.811886		0	
SQP 3	Start	End (5.0.0.5)	Low	High	
Inputs					
Hs2	1.5	1.5	0.5	1.5	
tr	0.3	0.3	0.1	0.35	
a2	2.8	2.771298561	0	5	
Ws1	0.8	0.918755908	0.5	1.5	
Ws2	0.6	0.713191787	0.5	1.5	
bw	2.5	2.5	1	4.5	
cw	0.24	0.235043405	0.2159	0.2921	
xw	0.8	0.693700801	0.1	1.5	
bh	0.6	0.5	0.5	2	
bv	0.9	1	0.2	1	
ch	0.275	0.220703783	0.1	0.6	
cv	0.08	0.05	0.05	0.6	
xh	1.6	1.6	1.5	2.13	
xv	1.6	1.6	1.5	2.13	
fail	0.8	0.867080935	0.1	0.9	
frud	0.8	0.797137786	0.1	0.9	
fele	0.8	0.801994263	0.1	0.9	
Hs1	1.4	1.469986672	0.5	1.5	
Outputs					
g1	264.718237	-96.833868		0	
g2	-1.157649	-1.627082		0	
g5	-0.883497	-0.882615		0	
g6	-0.798167	-0.797537		0	
g7	-0.712837	-0.712459		0	
g8	-0.627507	-0.627381		0	
g10	-0.456848	-0.457226		0	
g9	-0.542178	-0.542304		0	
g11	-0.371518	-0.372148		0	
g3	-0.237527	-0.276336		0	
g4	-0.520802	-0.520858		0	
g12	-0.286188	-0.28707		0	
g13	-0.13196	-0.03196		0	
g14	-3.917339	-0.753659		0	
g17	-0.061427	-0.004228		0	
g20	-0.439337	-0.355797		0	
g22	-2.208763	-1.702892		0	
g15	-34.238786	-42.851957		0	

g23	0.018469	-2.59E-04		0
g16	-0.0166	2.00E-04		0
g19	-0.439337	-0.355797		0
g24	-0.11564	-0.017559		0
g25	-0.11564	-0.199651		0
GOAL	-34.238786	-42.851957		

g18	-3.775159	-3.705476		0
g21	-2.208763	-1.702892		0
EGO 1	Start	End (13)	Low	High
Inputs				
Hs2	1.280443587	1.45166613	0.5	1.5
tr	0.263680112	0.10375665	0.1	0.35
a2	4.40257233	3.152243435	0	5
Ws1	0.675028469	0.844395878	0.5	1.5
Ws2	0.920328191	0.92810678	0.5	1.5
bw	3.083650271	2.906401651	1	4.5
cw	0.268524158	0.2159	0.2159	0.2921
xw	1.249768261	0.631978116	0.1	1.5
bh	1.941527534	0.5	0.5	2
bv	0.618339201	0.2	0.2	1
ch	0.375042198	0.6	0.1	0.6
cv	0.501110378	0.05	0.05	0.6
xh	1.614375665	2.13	1.5	2.13
xv	1.607131684	2.13	1.5	2.13
fail	0.202297414	0.9	0.1	0.9
frud	0.249495811	0.9	0.1	0.9
fele	0.188743182	0.9	0.1	0.9
Hs1	0.620410561	1.5	0.5	1.5
Outputs				
g1	955.430104	-547.395382		0
g2	-410.91579	-809.673536		0
g5	-0.085527	-0.08437		0
g6	-0.073697	-0.074117		0
g7	-0.061868	-0.063864		0
g8	-0.050038	-0.053611		0
g10	-0.026378	-0.033105		0
g9	-0.038208	-0.043358		0
g11	-0.014548	-0.022851		0
g3	-0.134701	-0.153227		0
g4	-0.523599	-0.517924		0
g12	-0.002718	-0.012598		0
g13	0.170029	-0.425558		0
g14	-20.660748	-3.47945		0
g17	-0.298692	0.009808		0
g20	-7.137466	-2.287921		0
g22	-7.716272	-0.358973		0
g15	39.656544	-55.313398		

g23	0.044218	-0.124961		0
g16	-0.3636	0.0371		0
g19	-0.988792	-2.287921		0
g24	-0.159914	-0.15385		0
g25	-0.159914	-0.15385		0
GOAL	39.656544	-55.313398		

g18	-0.988792	-4.659957		0
g21	-7.716272	-0.358973		0
EGO 2	Start	End (48)	Low	High
Inputs				
Hs2	1.312583622	1.5	0.5	1.5
tr	0.3043102	0.333047279	0.1	0.35
a2	0.469671468	3.858465156	0	5
Ws1	0.753219575	0.5	0.5	1.5
Ws2	0.803392209	0.5	0.5	1.5
bw	1.640722824	3.346379609	1	4.5
cw	0.26719959	0.2921	0.2159	0.2921
xw	0.674789484	1.454775714	0.1	1.5
bh	1.93553329	2	0.5	2
bv	0.96326396	0.2	0.2	1
ch	0.261931476	0.1	0.1	0.6
cv	0.281060231	0.498882682	0.05	0.6
xh	1.885423935	1.857605157	1.5	2.13
xv	1.862000183	1.5	1.5	2.13
fail	0.19368235	0.507253993	0.1	0.9
frud	0.558913241	0.418517144	0.1	0.9
fele	0.285743194	0.273065341	0.1	0.9
Hs1	0.703495109	1.5	0.5	1.5
Outputs				
g1	-0.065984	0.148914		0
g2	-18.577954	-3.656556		0
g5	-0.887541	-0.811947		0
g6	-0.861466	-0.687557		0
g7	-0.835391	-0.563166		0
g8	-0.809316	-0.438775		0
g10	-0.757167	-0.189994		0
g9	-0.783241	-0.314384		0
g11	-0.731092	-0.065603		0
g3	-0.394807	0.053872		0
g4	-0.523599	-0.519317		0
g12	-0.705017	0.058788		0
g13	-0.927973	0.01442		0
g14	79.121745	0.506805		0
g17	-0.233966	-0.357308		0
g20	-3.227055	-8.978726		0
g22	-6.215073	-0.608092		0
g15	6.500342	0.748231		

g23	-0.183824	-0.067945		0
g16	-0.7732	-0.0578		0
g19	-1.258148	-8.978726		0
g24	-0.207388	0.015419		0
g25	-0.207388	-0.287454		0
GOAL	6.500342	0.748231		

g18	-1.258148	-8.379968		0
g21	-6.215073	-0.608092		0
EGO 3	Start	End (207)	Low	High
Inputs				
Hs2	0.951474117	0.5	0.5	1.5
tr	0.305936934	0.35	0.1	0.35
a2	1.668392853	2.957480342	0	5
Ws1	1.494166094	0.978604155	0.5	1.5
Ws2	1.017955339	0.5	0.5	1.5
bw	3.779634472	2.394263399	1	4.5
cw	0.221763539	0.267620822	0.2159	0.2921
xw	0.180957851	0.757121385	0.1	1.5
bh	0.969307674	0.5	0.5	2
bv	0.266855812	1	0.2	1
ch	0.431780504	0.331940445	0.1	0.6
cv	0.559039051	0.05	0.05	0.6
xh	1.655991613	1.733630756	1.5	2.13
xv	1.538581005	1.50589167	1.5	2.13
fail	0.813824694	0.9	0.1	0.9
frud	0.243823016	0.9	0.1	0.9
fele	0.87043663	0.9	0.1	0.9
Hs1	1.365135172	1.492658277	0.5	1.5
Outputs				
g1	2261.523279	-459.567693		0
g2	-1.423621	-1.435548		0
g5	-0.65205	-0.901342		0
g6	-0.542885	-0.818348		0
g7	-0.433719	-0.735353		0
g8	-0.324554	-0.652358		0
g10	-0.106224	-0.486368		0
g9	-0.215389	-0.569363		0
g11	0.002941	-0.403373		0
g3	0.23465	-0.026944		0
g4	-0.515139	-0.503795		0
g12	0.112106	-0.320378		0
g13	0.51453	-0.137697		0
g14	-12.739665	-8.795344		0
g17	0.165641	-0.042255		0
g20	-0.682767	-0.279705		0
g22	-0.001457	-2.137208		0
g15	-55.69887	-36.138764		0

g23	0.758755	-0.014729		0
g16	0.1932	-0.0378		0
g19	-8.517808	-0.279705		0
g24	0.758755	-0.042039		0
g25	-1.115218	-0.181152		0
GOAL	-55.69887	-36.138764		

g18	-10.410888	-3.525178		0
21	-0.682767	-2.137208		0